

An Efficient k -modes Algorithm for Clustering Categorical Datasets

Karin S. Dorman and Ranjan Maitra

Mining clusters from datasets is an important endeavor in many applications. The k -means algorithm is a popular and efficient distribution-free approach for clustering numerical-valued data but can not be applied to categorical-valued observations. The k -modes algorithm addresses this lacuna by taking the k -means objective function, replacing the dissimilarity measure and using modes instead of means in the modified objective function. Unlike many other clustering algorithms, both k -modes and k -means are scalable, because they do not require calculation of all pairwise dissimilarities. We provide a fast and computationally efficient implementation of k -modes, OTQT, and prove that it can find superior clusterings to existing algorithms. We also examine five initialization methods and three types of K -selection methods, many of them novel, and all appropriate for k -modes. By examining the performance on real and simulated datasets, we show that simple random initialization is the best initializer, a novel K -selection method is more accurate than two methods adapted from k -means, and that the new OTQT algorithm is more accurate and almost always faster than existing algorithms.

Index Terms

categorical data clustering, initialization methods, Jump statistic, k -modes

I. INTRODUCTION

Identifying groups of similar observations in datasets is common in a wide array of applications with many methods developed in statistics, machine learning and the applied sciences [1]–[7]. The k -means algorithm [8]–[11] is arguably the most popular method for clustering numerical-valued observations, but it is inappropriate for datasets with categorical attributes.

There exist several methods for clustering categorical-featured datasets [12], but the most direct counterpart to k -means is the k -modes algorithm¹ [14], [15], where each cluster is characterized by its sample mode, rather than its sample mean, and the objective function is the sum of distances between the observations and their respective cluster modes. The [15] version of k -modes is more commonly implemented, and it mimics the [9] k -means algorithm [16]. It is initialized with k modes, and then alternately (a) allocates the next observation to the closest mode and (b) updates the affected modes, continuing to cycle through the observations until no change occurs during a complete pass. Since the mode of a subset is defined without reference to a distance metric, k -modes has been modified to use a variety of distinct distance metrics [17]–[20], but we focus on the original version that uses Hamming distances.

There have been variations proposed on MacQueen’s k -means algorithm, and some are provably superior algorithms. Lloyd’s algorithm [10] updates the means only *after all* the observations have been reallocated to the clusters, but there appears to be little practical difference with MacQueen’s algorithm [21], [22]. On the other hand, [23] only shifts an observation between clusters if the objective function improves, a change proven to achieve better optima [22]. Compared to MacQueen’s and Lloyd’s algorithms, Hartigan’s algorithm takes into account the distance of an observation to the means *after* the resulting changes in those means. Further efficiency tweaks avoid attempts to move observations to clusters that have not changed since the last pass through the data and a “quick-transfer stage,” where observations are only swapped between the two clusters with means closest to the observation [11]. Presumably, the quick-transfer stage rapidly calculates near-optimal improvements to the objective function that ultimately speed convergence.

The k -modes algorithm proposed by [14] follows the logic of Lloyd’s k -means algorithm, but to our knowledge no one has adapted Hartigan’s or Hartigan and Wong’s k -means algorithms to k -modes. We propose (Section II) an Optimal Transfer Quick-Transfer (OTQT) algorithm for k -modes analogous to Hartigan and Wong’s algorithm for k -means. A simpler variant, the Optimal Transfer (OT) algorithm, is more analogous to Hartigan’s algorithm. We also propose several initialization methods and K -selection algorithms for k -modes. We provide theoretical evidence that the proposed algorithms can achieve better optima than either previous k -modes algorithm. We also evaluate, in Section III, the performance of all methods on six test datasets, and more thoroughly in a moderately-sized simulation study. The paper concludes with some discussion. An appendix listing our software and additional figures to summarize our experimental results is included.

K. S. Dorman is with the Departments of Statistics and Genetics Development and Cell Biology at Iowa State University, Ames, Iowa, USA.

R. Maitra is with the Department of Statistics, Iowa State University, Ames, Iowa, USA.

This research was supported in part by the United States Department of Agriculture (USDA) National Institute of Food and Agriculture (NIFA) Hatch project IOW03617. The content of this paper however is solely the responsibility of the authors and does not represent the official views of either the NIFA or the USDA.

¹Another clustering algorithm with the same name [13] is intended for continuous data.

II. METHODOLOGY

A. Preliminaries

Let $\mathcal{X} = \{\mathbf{X}_1, \mathbf{X}_2, \dots, \mathbf{X}_n\}$ be a dataset of n observation records, where the i th record $\mathbf{X}_i = (X_{i1}, X_{i2}, \dots, X_{ip})$ has p categorical-valued features. The *weighted dissimilarity* between any two records \mathbf{X}_i and \mathbf{X}_j is determined by the number of mismatched features, or specifically,

$$\delta(\mathbf{X}_i, \mathbf{X}_j) = \sum_{\ell=1}^p \varpi_{\ell, X_{i\ell}, X_{j\ell}} \mathbb{1}(X_{i\ell} \neq X_{j\ell}), \quad (1)$$

where $X_{i\ell} \neq X_{j\ell}$ implies that $X_{i\ell}$ and $X_{j\ell}$ are in different categories and $\mathbb{1}(\cdot)$ is an indicator function taking an event and returning value 1 or 0 according to the truth of the event. When $\varpi_{\ell, X_{i\ell}, X_{j\ell}} \equiv 1$ for all i, j, ℓ , then (1) reduces to the Hamming distance, giving equal importance to each observation and category of an attribute. We use the Hamming distance in this paper, but there has been much discussion about alternative weights or distances [17], [18], [24]–[28].

The objective of k -modes is to minimize the summed distances of the observations to their assigned cluster modes. Letting

$$\Delta(\mathcal{X}, \boldsymbol{\mu}) = \sum_{i=1}^n \delta(\mathbf{X}_i, \boldsymbol{\mu}), \quad (2)$$

with $\delta(\cdot, \cdot)$ as in (1), [15] defines a mode of \mathcal{X} as the vector $\hat{\boldsymbol{\mu}} = (\hat{\mu}_1, \hat{\mu}_2, \dots, \hat{\mu}_p)$ which minimizes (2), *i.e.* $\hat{\boldsymbol{\mu}} = \operatorname{argmin}_{\boldsymbol{\mu}} \Delta(\mathcal{X}, \boldsymbol{\mu})$. Extending this concept to K clusters, k -modes must identify the partition $\mathcal{C} = \{\mathcal{C}_1, \mathcal{C}_2, \dots, \mathcal{C}_K\}$ of \mathcal{X} and modes $\boldsymbol{\mu}_1, \boldsymbol{\mu}_2, \dots, \boldsymbol{\mu}_K$, such that the objective function

$$\mathcal{W}_K = \sum_{k=1}^K \sum_{i=1}^n \mathbb{1}(\mathbf{X}_i \in \mathcal{C}_k) \delta(\mathbf{X}_i, \boldsymbol{\mu}_k) \quad (3)$$

is minimized. At the minimum value, $\hat{\boldsymbol{\mu}}_k$ is the mode of the observations in \mathcal{C}_k .

There are multiple optimization methods that could be developed to minimize (3). The k -modes algorithm of [15] starts with K initial modes $\boldsymbol{\mu}_1, \boldsymbol{\mu}_2, \dots, \boldsymbol{\mu}_K$ and iteratively minimizes (3):

- 1) For each $i = 1, 2, \dots, n$, allocate \mathbf{X}_i to the group with closest mode—that is, assign \mathbf{X}_i to cluster $\mathcal{C}_{\hat{k}}$ where $\hat{k} = \operatorname{argmin}_k \delta(\mathbf{X}_i, \boldsymbol{\mu}_k)$. Update $\boldsymbol{\mu}_k$ after each allocation, which by minimizing (2) is

$$\mu_{k\ell} = \operatorname{argmax}_{c \in \mathcal{J}_\ell} \sum_{j=1}^i \mathbb{1}(\mathbf{X}_j \in \mathcal{C}_k, X_{j\ell} = c), \quad (4)$$

for the ℓ th coordinate given the current observation i . We define a (possibly arbitrary) ordering of the distinct observed characters \mathcal{J}_ℓ at coordinate ℓ ; the mode is assigned the low rank category when there is a tie, guaranteeing its uniqueness.

- 2) For each $i = 1, 2, \dots, n$, move \mathbf{X}_i from the current group k to another cluster k' if it is closer to $\boldsymbol{\mu}_{k'}$ than $\boldsymbol{\mu}_k$. After each reallocation, update $\boldsymbol{\mu}_{k'}$ and $\boldsymbol{\mu}_k$ using (4) with upper limit $i = n$ on the sum.
- 3) Repeat Step 2 until there are no reassignments during a full cycle through the dataset.

This algorithm updates $\boldsymbol{\mu}_k$ after every allocation, including after each initial assignment in the first iteration. Later, we introduce initialization schemes that do not update the modes during the first iteration. It can be important, especially when updating modes during the first iteration, to shuffle the observation input order before starting the algorithm, since we have observed pathological orderings that fail to achieve the global minimum no matter which algorithm or initialization method is used.

B. A New, More Efficient k -Modes Algorithm

[11] make two major improvements on the [9] algorithm for k -means: (1) they verify that the objective function will improve before moving an observation between clusters, and (2) they avoid attempting any move with no hope to improve the objective function. They also propose a heuristic *quick-transfer stage*, where only transfers between clusters with the closest and the putative next closest means are considered. We provide a new k -modes algorithm in the spirit of [11].

Along with the modes $\boldsymbol{\mu}_1, \boldsymbol{\mu}_2, \dots, \boldsymbol{\mu}_K$, we also define the *minor modes* $\mathbf{m}_1, \mathbf{m}_2, \dots, \mathbf{m}_K$, where

$$m_{k\ell} = \operatorname{argmax}_{\substack{c \in \mathcal{J}_\ell \\ c \neq \mu_{k\ell}}} \sum_{j=1}^n \mathbb{1}(\mathbf{X}_j \in \mathcal{C}_k, X_{j\ell} = c)$$

for $1 \leq k \leq K$. Further, we will maintain up-to-date counts of category c at coordinate ℓ in cluster k : $n_{k\ell c}$. From these counts, we can quickly compute the k th mode, using $\mu_{k\ell} = \operatorname{argmax}_{c \in \mathcal{J}_\ell} n_{k\ell c}$, and the k th minor mode, using $m_{k\ell} = \operatorname{argmax}_{c \in \mathcal{J}_\ell, c \neq \mu_{k\ell}} n_{k\ell c}$.

Before describing the algorithm, we first state and prove the cost of moving an observation from cluster \mathcal{C}_k to cluster $\mathcal{C}_{r'}$. An important observation emerging from this proof is that there are two types of sites that determine whether a move will take place:

- 1) A site that favors the move is one where $X_{i\ell}$ is or becomes the mode in cluster \mathcal{C}_r by breaking a tie *and* was not or lost mode status by breaking a tie in cluster \mathcal{C}_k .
- 2) A site that disfavors the move is one where $X_{i\ell}$ is not or becomes the mode in cluster \mathcal{C}_r by creating a tie *and* was or lost the mode status by creating a tie in cluster \mathcal{C}_k .

All other sites are irrelevant, and if there are more sites of type 1 than type 2, then X_i will move from \mathcal{C}_k to \mathcal{C}_r . Additional claims and proofs to support the superiority of the proposed algorithm are discussed in Results §III-B.

Claim II-B.1. *The cost of moving observation X_i from cluster \mathcal{C}_k to \mathcal{C}_r is*

$$\sum_{\ell=1}^p [\mathbb{1}(n_{r\ell\mu_{r\ell}} \geq n_{r\ell X_{i\ell}} + 1) - \mathbb{1}(X_{i\ell} = \mu_{k\ell}, n_{k\ell\mu_{k\ell}} = n_{k\ell m_{k\ell}}) - \mathbb{1}(X_{i\ell} \neq \mu_{k\ell})].$$

Proof. We consider all possible changes at coordinate ℓ when moving X_i from cluster k to r . In these descriptions, counts, such as $n_{k\ell j}$, modes $\mu_{k\ell}$ and minor modes $m_{k\ell}$ refer to the counts, modes, and minor modes *before* the move. In addition, we make heavy use of the possibly arbitrary ordering of the elements in \mathcal{J}_ℓ observed at site ℓ . In italics, we highlight the conditions that lead to a change either in the cost of cluster \mathcal{C}_r or the cost of cluster \mathcal{C}_k . Compare these italicized conditions to the three events indicated in the equation to complete the proof.

We consider the three possible outcomes at coordinate ℓ of moving X_i to cluster \mathcal{C}_r : either $X_{i\ell}$ is already the mode, $X_{i\ell}$ is not the mode and will not become the mode, or $X_{i\ell}$ is not the mode, but will become the mode. Clearly, if $X_{i\ell} = \mu_{r\ell}$ is already the mode, then adding X_i only increases the support for the mode and there is no cost of adding X_i to cluster \mathcal{C}_r at site ℓ . *If the mode $\mu_{r\ell} \neq X_{i\ell}$ and adding $X_{i\ell}$ does not change the mode $\mu_{r\ell}$, then there will be a cost of 1 at coordinate ℓ for adding $X_{i\ell}$ to cluster \mathcal{C}_r . This situation occurs if $\mu_{r\ell}$ is observed more often than $X_{i\ell}$ in cluster \mathcal{C}_r , even after adding X_i , i.e., $n_{r\ell\mu_{r\ell}} > n_{r\ell X_{i\ell}} + 1$, or $n_{r\ell\mu_{r\ell}} = n_{r\ell X_{i\ell}} + 1$, but $\mu_{r\ell} < X_{i\ell}$.* Finally, if addition of X_i changes the mode at site ℓ , it can be because $X_{i\ell} = m_{r\ell}$ is a minor mode and $n_{r\ell\mu_{r\ell}} = n_{r\ell m_{r\ell}}$ (with ordering $\mu_{r\ell} < X_{i\ell}$), and the cost does not change as there were $n_{r\ell m_{r\ell}}$ mismatches before and there will be an equal $n_{r\ell\mu_{r\ell}}$ mismatches after the change. *Addition of X_i can also change the mode if $n_{r\ell\mu_{r\ell}} = n_{r\ell X_{i\ell}} + 1$ and $X_{i\ell} < \mu_{r\ell}$, in which case the cost increases by 1 because there were $n_{r\ell X_{i\ell}}$ mismatches before the change, but there will be $n_{r\ell\mu_{r\ell}} = n_{r\ell X_{i\ell}} + 1$ mismatches after the change.*

Meanwhile, there are three possible outcomes of moving X_i out of cluster \mathcal{C}_k : either $X_{i\ell}$ is not the mode, it is the mode and will stay the mode, or it is the mode and the mode will change. *If $X_{i\ell} \neq \mu_{k\ell}$ is not the mode, it cannot become the mode upon X_i 's departure, and the cost will reduce by 1 when X_i departs.* If $X_{i\ell} = \mu_{k\ell}$ is the mode and the mode does not change, it is because $n_{k\ell\mu_{k\ell}} > n_{k\ell m_{k\ell}} + 1$ or $n_{k\ell\mu_{k\ell}} = n_{k\ell m_{k\ell}} + 1$ and $\mu_{k\ell} < m_{k\ell}$. In both cases, the cost does not change. Finally, there are two ways for $X_{i\ell} = \mu_{k\ell}$ to lose mode status upon departure of X_i . If $n_{k\ell\mu_{k\ell}} = n_{k\ell m_{k\ell}} + 1$ and $m_{k\ell} < \mu_{k\ell}$, then $m_{k\ell}$ will become the mode, but the new cost will be $n_{k\ell\mu_{k\ell}} - 1 = n_{k\ell m_{k\ell}}$, the old cost. *Otherwise if there is a tie $n_{k\ell\mu_{k\ell}} = n_{k\ell m_{k\ell}}$ for the mode and $X_{i\ell} < m_{k\ell}$, then X_i 's departure will make $m_{k\ell}$ the mode. The new cost will be $n_{k\ell\mu_{k\ell}} - 1 = n_{k\ell m_{k\ell}} - 1$, 1 less than the previous cost.* \square

Let the “live set” of clusters be those that have experienced a change in membership during the last cycle through the observations. We additionally define the “cost set” as the collection of clusters whose membership costs (contribution to objective function (3)) need to be recalculated. Given a set of k modes obtained by some initialization procedure, the OTQT algorithm is:

- 1) **Getting started.** For each observation $X_i, i = 1, 2, \dots, n$, find the two closest modes μ_k and μ_r . Assign X_i to the cluster \mathcal{C}_k with closest mode μ_k , which is then updated. If there is a tie with μ_k and $\mu_r, k < r$, we assign the observation to μ_k . Place all clusters in the live and cost sets. Compute the minor modes. At this time, the modes and minor modes for each group are correct, but the two closest modes to each observation have not been updated after the assignment of subsequent observations. As the algorithm progresses, the closest and second closest mode information will improve.
- 2) **Optimal transfer (OT) stage.** Loop through all observations. For an observation X_i in cluster k :
 - a) If k is in the cost set, recompute the cost of X_i 's membership in cluster k as

$$\sum_{\ell=1}^p [\mathbb{1}(X_{i\ell} = \mu_{k\ell}, n_{k\ell\mu_{k\ell}} = n_{k\ell m_{k\ell}}) + \mathbb{1}(X_{i\ell} \neq \mu_{k\ell})]. \quad (5)$$

From the proof, membership of X_i in cluster k at coordinate ℓ has a non-zero cost if $X_{i\ell}$ is a non-modal category or if $X_{i\ell}$'s introduction into the cluster induces a new mode at coordinate ℓ .

- b) Now check the cost of moving X_i , while applying a branch-and-bound algorithm to reduce computational cost. Specifically, we first check the cost of moving X_i to the recorded second-closest mode, if it is live. We also check the cost of moving X_i to all other live clusters, aborting the calculation as soon as it exceeds the previous lowest cost. The cost of adding X_i to $\mathcal{C}_r, r \neq k$ is

$$\sum_{\ell=1}^p \mathbb{1}(n_{r\ell\mu_{r\ell}} \geq n_{r\ell X_{i\ell}} + 1). \quad (6)$$

If the minimum of these costs is less than the cost of membership in the current \mathcal{C}_k or the costs are equal and the new cluster index $r < k$, **transfer** X_i from the old \mathcal{C}_k to the new \mathcal{C}_r :

- Put \mathcal{C}_k and \mathcal{C}_r in both the live and distance sets.
 - Assign μ_r as the closest mode and μ_k as the second closest mode to X_i .
 - For each coordinate ℓ , increase $n_{r\ell X_{i\ell}}$ and decrease $n_{k\ell X_{i\ell}}$ by one.
 - We may need to update the source cluster's mode μ_k and minor mode m_k . For each coordinate ℓ ,
 - If $X_{i\ell} = \mu_{k\ell}$, $n_{k\ell\mu_{k\ell}} = n_{k\ell m_{k\ell}}$ and $m_{k\ell} < \mu_{k\ell}$, set $\mu_{k\ell} = m_{k\ell}$ and $m_{k\ell}$ to the lowest ranked category c with $m_{k\ell} < c \leq X_{i\ell}$ and $n_{k\ell c} = n_{k\ell m_{k\ell}}$.
 - If $X_{i\ell} = \mu_{k\ell}$ and $n_{k\ell\mu_{k\ell}} = n_{k\ell m_{k\ell}} - 1$, then set $\mu_{k\ell} = m_{k\ell}$. Search through categories to set $m_{k\ell}$. It will be the first category $c > m_{k\ell}$ with $n_{k\ell c} = n_{k\ell m_{k\ell}}$ or, if the former does not exist, then the first category $c \leq X_{i\ell}$ with $n_{k\ell c} = n_{k\ell X_{i\ell}}$.
 - Otherwise, if $X_{i\ell} = m_{k\ell}$, then search through \mathcal{J}_ℓ to detect a possible new $m_{k\ell}$.
 - We may also need to update the target clusters's mode μ_r and minor mode m_r . For each coordinate ℓ ,
 - If $n_{r\ell X_{i\ell}} > n_{r\ell\mu_{r\ell}}$ or $n_{r\ell X_{i\ell}} = n_{r\ell\mu_{r\ell}}$ and $X_{i\ell} < \mu_{r\ell}$, then set $m_{r\ell} = \mu_{r\ell}$ and $\mu_{r\ell} = X_{i\ell}$.
 - Otherwise, if $n_{r\ell X_{i\ell}} > n_{r\ell m_{rj}}$ or $n_{r\ell X_{i\ell}} = n_{r\ell m_{rj}}$ and $X_{i\ell} < m_{r\ell}$, then set $m_{r\ell} = X_{i\ell}$.
- c) The algorithm terminates as soon as the live set is empty. Otherwise, remove all clusters from the cost set, and remove all clusters not involved in a transfer from the live set.

The rule for breaking ties guarantees the same solution given the same initial modes in the same order, but may yield different clusters when the same initial modes are given in different order. To guarantee the same solution despite mode ordering, the rule could be modified to transfer only when the costs are equal and $\mu_r < \mu_k$, by an induced ordering on the modes. However, such a rule would create a bias, always assigning observations to the lower rank mode when there are observations equidistant to multiple modes in the final solution, and not reflecting the true ambiguity in the data.

- 3) **Quick transfer (QT) stage.** Repeatedly loop through all observations. For any observation X_i in cluster k :
- a) Recompute the cost of X_i 's current membership by (5) if k is in the live set.
 - b) If either the cluster \mathcal{C}_k with the closest mode or \mathcal{C}_r with the second closest mode are in the live set, compute the cost of joining \mathcal{C}_r by (6). If the cost to join \mathcal{C}_r is less than the cost of membership in k , carry out transfer step 2b, but do not place \mathcal{C}_k or \mathcal{C}_r in the distance set.
 - c) If there has been no transfer for the last n observations, go to the Optimal Transfer Stage (step 2).

The OTQT algorithm just described alternates between OT and QT stages, but since the purpose and value of the QT stage is unclear [11], we also consider algorithm OT, which iterates the OT stage without passage through the QT stage. Meanwhile, we will use H97 to refer to the k -modes algorithm of [15].

1) *Some Theoretical Results:* We now provide some theoretical understanding of how the OT algorithm works. We prove it is monotone and guaranteed to terminate in a finite number of iterations. We show that the clusters are nonempty and maintain distinct modes at each iteration. Finally, we show that the set of moves made by H97 is a strict subset of the moves made by OT.

Claim II-B.2. *The OT algorithm initialized with $K \leq n$ distinct observations has the following properties:*

- 1) *The objective function value \mathcal{W}_K decreases at every iteration.*
- 2) *The algorithm terminates after finitely many iterations.*
- 3) *The partition will have no empty clusters at any iteration.*
- 4) *The modes will remain distinct at every iteration.*

Proof. 1) The algorithm terminates unless there is an observation X_i whose move from cluster \mathcal{C}_k to \mathcal{C}_r will reduce the objective function \mathcal{W}_K by at least 1, so Property 1 holds.

- 2) The objective function is bounded $0 \leq \mathcal{W}_K \leq (n - K)p$, where n is the number of observations and p is the number of coordinates. Thus, the initial value of the objective function is finite, and the algorithm must terminate in finitely many steps.
- 3) We distinguish empty clusters introduced during initialization vs. later iterations. Recall that during initialization and subsequent iterations, we process the observations in their index order.

There cannot be an empty cluster after the first iteration if there are no updates during the first iteration. If there are updates, each update occurs *after* an observation is assigned to the cluster. To get an empty cluster, there must be a cluster \mathcal{C}_k whose mode is updated to match that of \mathcal{C}_r *before* any observations are added to \mathcal{C}_r . Then, even the observation that seeded \mathcal{C}_r will get assigned to \mathcal{C}_k if $k < r$. WOLOG, suppose adding X_i to \mathcal{C}_k precipitates a change in μ_k to match μ_r . This is a contradiction because before the addition, there must exist a site ℓ in μ_k where $\mu_{k\ell} \neq X_{i\ell}$, costing 1, but $\mu_{r\ell} = X_{i\ell}$ costs nothing. Apart from such sites, all other sites in μ_k and μ_r either both match or both mismatch X_i , and thus do not change the distance.

To form an empty cluster at a later iteration, its last member must move to a new cluster. Since the cost of membership of this last member is 0, there can be no lower or equal cost of membership in any other cluster, unless there is another cluster with an identical mode. Claim 4 disallows the possibility of equal modes.

- 4) The argument in proving 3 also guarantees K distinct modes *after the first iteration*, which we will use in the following proof. We separate the proof below into separate cases for $K = 2$ and $K > 2$ modes.

If $K = 2$, then the modes will remain distinct. For X_i to move between two clusters, there must be at least one site ℓ where $X_{i\ell}$ is or becomes the mode in the receiving cluster (without tie), but was not so or loses mode status by breaking a tie in the source cluster (see Claim II-B.1), which contradicts the possibility of equal modes after the move.

For $K > 2$, suppose that we obtain two equal modes by moving observation X_i from cluster \mathcal{C}_k to \mathcal{C}_s such that after the move $\mu_k = \mu_r$ or $\mu_s = \mu_r$ for some $r \notin \{k, s\}$. At the time of the move, this configuration implies that the minor mode $m_k = \mu_r$ or $m_s = \mu_r$, and that there exists a nonempty subset \mathcal{L} of sites where there is a tie or about to be one with the mode state in \mathcal{C}_k or \mathcal{C}_s , WOLOG \mathcal{C}_k . Such sites are said to be in the *cuspl state*. If $\ell \in \mathcal{L}$, then the mode and minor mode are tied ($n_{k\ell m_{k\ell}} = n_{k\ell \mu_{k\ell}}$ with $\mu_{k\ell} < m_{k\ell}$) or nearly tied ($n_{k\ell m_{k\ell}} = n_{k\ell \mu_{k\ell}} + 1$ with $m_{k\ell} < \mu_{k\ell}$). For sites $\ell \notin \mathcal{L}$, the plurality of observations in \mathcal{C}_k must match $\mu_{s\ell}$.

To create the cuspl state at $\ell \in \mathcal{L}$ in cluster k during initialization, we must add an observation X_j to cluster k although $X_{j\ell} \neq \mu_{k\ell}$. If X_j is to go to cluster k instead of any other cluster h , it does so either because of a **tie resolution** or a **driving difference**. A **tie resolution** occurs if $\delta(X_j, \mu_k) \leq \delta(X_j, \mu_h)$ for all h and equality is achieved for some h , but $k \leq h$ for all such h . In particular, if $\delta(X_j, \mu_k) = \delta(X_j, \mu_r)$ for ultimately tied cluster r , either $X_{j\ell} \neq \mu_{r\ell} \neq \mu_{k\ell}$ or $X_{j\ell} = \mu_{r\ell} \neq \mu_{k\ell}$. In the first case, ℓ may end up in the cuspl state, but $m_{k\ell} = \mu_{r\ell}$ cannot be true, as required. In the second case, there must exist another site $\ell_1 \neq \ell$, where $X_{j\ell_1} = \mu_{k\ell_1} \neq \mu_{r\ell_1}$. The second case also arises if X_j is assigned to k instead of r because of a **driving difference** making $\delta(X_j, \mu_k) < \delta(X_j, \mu_r)$. Since $X_{j\ell} \neq \mu_{k\ell}$, there must be sites elsewhere, in particular some ℓ_1 , where $X_{j\ell_1} = \mu_{k\ell_1} \neq \mu_{r\ell_1}$. If $\ell_1 \in \mathcal{L}$, then it cannot yet be in the cuspl state because it was already the mode in cluster k prior to the move. Otherwise, if $\ell_1 \notin \mathcal{L}$, then $\mu_{k\ell_1} \neq \mu_{r\ell_1}$. Thus, after addition of X_j , clusters k and r are not in the desired configuration. Subsequent additions required to achieve the desired configuration follow a similar pattern.

To create the desired configuration after initialization, we must add to *or retain in* cluster k an observation X_j even though $X_{j\ell} \neq \mu_{k\ell}$ *after* the move. Whether we add or retain X_j in cluster k is mostly semantic: retaining X_j is equivalent to removing it and adding it back. The **driving sites** that determine whether we add X_j to cluster k as opposed to any other cluster h are those that match the mode in cluster k or become the mode in cluster k by *breaking a tie*. Any site $\ell \in \mathcal{L}$ cannot be a driving site for cluster k , for then $\mu_{k\ell} = X_{j\ell}$ after the move. Therefore, there is no driving site or there is another driving site $\ell_1 \notin \mathcal{L}$. If there is no driving site, then X_j must already be in cluster k , but the final configuration has not been achieved (see below). Otherwise, site ℓ may end in the desired configuration but $\mu_{k\ell_1} \neq \mu_{r\ell_1}$.

We have been able to put cluster k in the cuspl state, but $\mu_{k\ell_1} \neq \mu_{r\ell_1}$ for some $\ell_1 \notin \mathcal{L}$ (Case A) or $m_{k\ell} \neq \mu_{r\ell}$ for some $\ell \in \mathcal{L}$ (Case B). We address each case separately.

Case A: To achieve the final state, we must add or retain X_j in cluster r even though $X_{j\ell_1} = \mu_{k\ell_1}$. Therefore, ℓ_1 may be a driving site for moving X_j to cluster k , but not to r . Whether a driving site or not, there must exist another driving site ℓ_2 to drive or retain X_j in cluster r . Such sites contradict the final configuration unless X_j is in cluster k and $X_{j\ell_2}$ is not the mode in cluster k or loses the mode status by breaking a tie, but both contradict the presumption that cluster k is already in the cuspl state.

Case B: If cluster k is in the cuspl state, but $\mu_{r\ell} \neq m_{k\ell}$, then cluster r must attain or be already in the same cuspl state as cluster k at site ℓ . However, cluster k achieved the cuspl state at site ℓ through a tie resolution in order to be in Case B. It is therefore impossible for cluster r to achieve the same cuspl state without additional driving sites.

In all cases, it is impossible to achieve the configurations that are one step away from achieving equal modes. Thus, it is impossible to achieve equal modes. □

Our next claim demonstrates that given a starting configuration, there exist scenarios where H97 will stop, but OT will continue and improve the optimum value of the objective function. For these initializations, algorithm OT will obtain a higher maximum, thus supporting our empirical observations.

Claim II-B.3. *There exist moves X_i from \mathcal{C}_k to \mathcal{C}_r that algorithm OT will take, but H97 will not.*

Proof. For observation X_i to move from \mathcal{C}_k to \mathcal{C}_r , there must exist at least one site ℓ where $X_{i\ell}$ is or breaks a tie to become the mode in cluster \mathcal{C}_r and $X_{i\ell}$ was not or broke a tie to lose the mode status in cluster \mathcal{C}_k . If at least one of these sites was already the mode in \mathcal{C}_r and was already not the mode in \mathcal{C}_k , then $\delta(X_i, \mu_k) > \delta(X_i, \mu_r)$ and H97 will take the move. However, if all these sites break a tie to become the mode in \mathcal{C}_r or break a tie to lose mode status in \mathcal{C}_k , then $\delta(X_i, \mu_k) \leq \delta(X_i, \mu_r)$ and H97 will not take the move. □

C. Initialization

The k -modes algorithm is iterative and starts with K initial modes $\tilde{\mu}_1, \tilde{\mu}_2, \dots, \tilde{\mu}_K$ that have a large impact on the achieved minimum. There have been several initialization methods proposed to select initial modes from among the observations \mathcal{X} , and we implement some of the existing methods along with our modifications in order to compare their performance. Our goal is to reach the global minimum of the k -modes objective function (3) through repeated random initialization, so we focus on stochastic initializers.

- **klar.** [15] proposed a simple initialization scheme that uses the first K observations as the initial modes. If the observations are randomly ordered, then this initialization method becomes stochastic and equivalent to random choice of K modes from the n observations as employed in the R package `klar`. We and `klar` insist the modes are distinct.
- **py.** This method, also due to [15], attempts to select distinct modes built from common categories at each coordinate. [29] interpreted this method as proposing $\mu'_{k\ell}$ by randomly sampling $c \in \mathcal{J}_\ell$ with probability proportional to its frequency $n_{\ell c} := \sum_{k=1}^K n_{k\ell c}$. Then to avoid null clusters, the algorithm assigns $\tilde{\mu}_k = \operatorname{argmin}_{\mathbf{X}_i \in \mathcal{X}} \delta(\mathbf{X}_i, \mu'_k)$ to be the closest observation to the proposal. The process is repeated if the selected observation is identical to a previously selected mode.
- **h97r.** We modify **py** and randomly sample $\mu'_{k\ell}$ from \mathcal{J}_ℓ with probability $\frac{1}{|\mathcal{J}_\ell|}$ for all $1 \leq \ell \leq p$.
- **clbr.** [30] proposed a deterministic initialization scheme that starts by computing an approximate density

$$d(\mathbf{X}_i) = \frac{1}{np} \sum_{\ell=1}^p n_{\ell X_{i\ell}} \quad (7)$$

around each observation i . The first mode $\tilde{\mu}_1 = \operatorname{argmax}_{1 \leq i \leq n} d(\mathbf{X}_i)$ is the most dense observation. Let \mathcal{S} , initialized to $\{\tilde{\mu}_1\}$, be the current set of modes. Then, defining

$$\delta(\mathbf{X}_i, \mathcal{S}) = \min_{\mathbf{s} \in \mathcal{S}} \delta(\mathbf{X}_i, \mathbf{s}), \quad (8)$$

the k th mode is

$$\tilde{\mu}_k = \operatorname{argmax}_{\mathbf{X}_i \in \mathcal{X}} d(\mathbf{X}_i) \delta(\mathbf{X}_i, \mathcal{S}),$$

given the current set of $k-1$ modes. The process is repeated until there are K modes in \mathcal{S} . We randomize this method by choosing the subsequent modes with probability proportional to $d(\mathbf{X}_i) \delta(\mathbf{X}_i, \mathcal{S})$.

- **km++.** We adapt the popular k -means++ initialization scheme for k -means [31] to k -modes as follows. The first mode is chosen at random. Subsequent modes are chosen proportional to the $\delta(\mathbf{X}_i, \mathcal{S})$ defined in (8) given the current mode set \mathcal{S} . We have also implemented a greedy version of this algorithm [31], but do not study it here.

In addition, there are competing methods for conducting the first cycle through the observations. [15] suggests updating the initial modes as observations are first assigned to clusters, but [14] does not. We implement both variants for each initialization method, appending ‘n’ to the initialization method name (e.g., **km++n**), if modes are *not* updated during the first cycle.

D. Choosing K

We consider ten methods for choosing K . Both the jump statistic [32] and the [33] statistic (called the KL statistic here) can be adapted to k -modes. Our jump statistic for supporting K clusters is

$$J_K = \widehat{\mathcal{W}}_K^{-Y} - \widehat{\mathcal{W}}_{K-1}^{-Y},$$

where $Y > 0$ is recommended to be $p/2$ and $\widehat{\mathcal{W}}_K$ is the distortion, or minimized objective function (3), when there are K clusters. Our KL statistic is

$$KL_K = \left| \frac{(K-1)^{2/p} \widehat{\mathcal{W}}_{K-1} - K^{2/p} \widehat{\mathcal{W}}_K}{K^{2/p} \widehat{\mathcal{W}}_K - (K+1)^{2/p} \widehat{\mathcal{W}}_{K+1}} \right|.$$

Both methods advocate choosing the K that maximizes the respective statistic.

The theory behind the jump statistic assumes equally probable clusters. We consider weighting the distortion in the jump statistic in two ways to account for unequally sized clusters. First, define a weighted version of the distortion function

$$\mathcal{W}_K = \sum_{k=1}^K w_k \sum_{i=1}^n \mathbb{1}(\mathbf{X}_i \in \mathcal{C}_k) \delta(\mathbf{X}_i, \tilde{\mu}_k). \quad (9)$$

The jump statistic defines $w_k = 1$ for all $k = 1, 2, \dots, K$. We define the iJump (iJ) statistic, where

$$w_k = \frac{n}{K \sum_{i=1}^n \mathbb{1}(\mathbf{X}_i \in \mathcal{C}_k)},$$

and the hJump (hJ) statistic, where

$$w_k = K \frac{\frac{1}{\sum_{i=1}^n \mathbb{1}(\mathbf{X}_i \in \mathcal{C}_k)}}{\sum_{l=1}^K \frac{1}{\sum_{i=1}^n \mathbb{1}(\mathbf{X}_i \in \mathcal{C}_l)}}.$$

iJ uses the inverse of the arithmetic mean proportions for the weights, while hJ uses the inverse of the harmonic mean proportions. We refer to K selected by these jump statistics as \hat{K}_J , \hat{K}_{iJ} , and \hat{K}_{hJ} . We use the same distortion functions in the KL statistic, selecting \hat{K}_{KL} , \hat{K}_{iKL} , and \hat{K}_{hKL} .

We find that all variants of the jump statistic can select K too large, appearing to pick up spurious signals when the sample size is small. [32] suggested estimating the uncertainty in the jump statistic by the bootstrap. They resample the data with replacement, minimize the objective function for different K , and estimate the bootstrap jump statistic. We introduce a novel, rapid bootstrap to assess when a jump statistic is indistinguishable from 0. To avoid reoptimizing the criterion for each resampled dataset, we condition on the contribution $\delta(\mathbf{X}_i, \mu_k)$ of observation \mathbf{X}_i to its cluster k and simply resample these contributions. In this way, we obtain bootstrapped distortions $\hat{\mathcal{W}}_{K-1}^{(b)}$ and $\hat{\mathcal{W}}_K^{(b)}$ and corresponding bootstrapped jump statistics $J_K^{(b)}$. We discard K from consideration if the 25th permille of the bootstrapped jump statistics is 0 or below. In all our analyses, the number of bootstrap replications $B = 1000$. We refer to these 0-truncated versions as J_t , iJ_t , hJ_t , with \hat{K}_{J_t} , \hat{K}_{iJ_t} , and \hat{K}_{hJ_t} the selected K obtained by choosing the maximum jump statistic that is distinguishable from 0 using the various weighting schemes. If no jump statistic is distinguishable from 0, the selected \hat{K}_{*t} is undefined.

Both the jump and KL statistics assume p independent coordinates. To approximate the number of independent coordinates in the real data, we form the design matrix \mathbf{X} from the observations \mathcal{X} and find the number n_e of eigenvalues explaining 99.9% of the variation in the data. Then, $p' = \frac{n_e p}{\text{rank}(\mathbf{X})}$ is used in place of p in the jump and KL statistics. (We use this p' in our calculations.)

During our simulation study, we observed that timing differences between initializations with and without updates in the first iteration were highly informative on the number of clusters. We turn this observation into a novel K -selection method. Given an algorithm and an initialization method, let T_{kui}, T_{kni} be the i th wait time to achieve the target optimum (we use the 5th quantile of all achieved optima, which is discussed further in §III-A3) with and without update during the first iteration when $K = k$. Then, our tenth K -selection method is simply

$$\hat{K}_{DM} = \arg \max_k \bar{T}_{ku} / \bar{T}_{kn},$$

where DM stands for the Daneel method². The results presented here use initialization method **klar**, because it was the fastest initializer.

III. PERFORMANCE EVALUATIONS

In all the comparative experiments, H97 is the k -modes algorithm of [15], while OTQT and OT refer to the proposed algorithms. In addition, we have five initialization methods **klar**, **py**, **h97r**, **clbr**, and **km++**, along with their variants, **klarn**, **pyn**, **h97rn**, **clbrn**, and **km++n**, where the modes are not updated during the first iteration. Further, there are 10 K -selection methods, the jump statistics, J , iJ , hJ , the 0-truncated jump statistics, J_t , iJ_t , hJ_t , the KL-statistics, KL , iKL , hKL , and the novel Daneel method DM.

A. Experimental Framework

TABLE I

REAL-WORLD DATASETS. HERE, n IS NUMBER OF OBSERVATIONS, p IS THE NUMBER OF NON-CONSTANT COORDINATES, p' IS THE NUMBER OF DIMENSIONS EXPLAINING 99.9% OF THE DATASET VARIATION, K_t IS THE REPORTED TRUE NUMBER OF CLUSTERS, $c = \sum_j (a_j - 1)$, WHERE a_j IS THE NUMBER OF CATEGORIES OBSERVED AT COORDINATE $1 \leq j \leq p$, AND ARI IS THE MEAN ADJUSTED RAND INDEX [34] FOR THE BEST SOLUTIONS AT THE INDICATED NUMBER OF CLUSTERS. THE MAXIMUM ARI IS BOLDFORED FOR EACH DATASET, BUT IF THE MAXIMUM DID NOT OCCUR FOR $K \in \{K_t - 1, K_t, K_t + 1\}$, WE REPORT THE MAXIMUM ARI AND THE MAXIMIZING K IN PARENTHESES UNDER COLUMN MAX.

Dataset	Abbr.	Data Dimensions					ARI			
		n	p	p'	K_t	c	$K_t - 1$	K_t	$K_t + 1$	max
cancer	c	699	8	7.8	2	72	0	0.67	0.39	–
mushroom	m	8,124	20	15.0	2	92	0	0.61	0.21	–
senators	se	100	542	49.9	3	1011	0.04	0.45	0.49	–
soybean	so	47	21	15.5	4	40	0.65	0.95	0.79	–
splice	sp	3,175	60	59.3	3	182	0.01	0.02	0.03	0.05 (7)
zoo	z	101	16	14.5	7	26	0.63	0.66	0.63	0.83 (5)

1) *Real-World Data*: We use six real-world categorical datasets to test the developed methods (Table I). Five of the datasets are from the UCI Machine Learning Repository [35]. The breast cancer (c) dataset contains missing information at one

²R. Daneel Olivaw was science fiction author Isaac Asimov's most famous robot, lending an appropriate name for this circuit-driven criterion.

coordinate, which we drop prior to our analysis³. The mushroom (m) dataset contains missing information at one coordinate and no variation at a second: we drop both coordinates prior to analysis. The soybean (so) dataset, which is the *small* soybean dataset from the repository, contains 14 coordinates with no variation, which we drop prior to our analysis. The zoo (z) dataset includes one numeric coordinate, number of legs, which we treat as categorical. The senators dataset (se) [36] is the voting patterns of 100 senators in the 109th US Congress from the January 3, 2005 to January 3, 2007. This dataset has 542 coordinates, each of which has three categories (voting for, against, or no vote recorded). There were nominally three groups of senators (44 Democrats, 1 Independent and 55 Republicans), so $K = 3$, however, the independent senator caucused with the Democratic senators during this Congress.

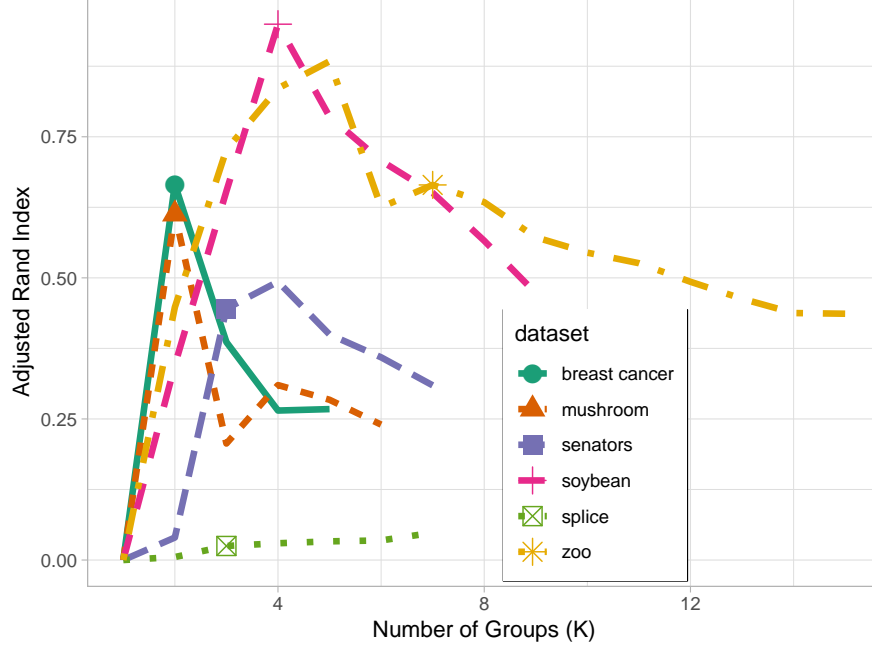


Fig. 1. The mean achieved ARI at each tested number of clusters K . The single point along each trajectory indicates the reported true K_t .

To characterize the strength of the clustering signal in these datasets, we compute the average adjusted Rand index [34] (ARI in Table I) for all solutions, regardless of algorithm or initialization method, that achieved the global minimum for a specified K . Since we do not know the true global minimum, we assume the minimum achieved criterion across all runs is the global minimum. Except in the splice dataset for $K > 2$, the observed minimum is achieved several times. The ARI for solutions achieving the global minimum may vary because the optimization function is discrete and there is randomness in the clustering of observations with tied distances to more than one mode. Four datasets achieved a maximal ARI at or near the reported true number of clusters K_t (Fig. 1). The splice dataset achieved a maximum ARI of 0.05 at $K = 7$, well above the reported value of $K_t = 3$. The low ARI values indicate little to no structure in the splice data, at least no structure consistent with the stated labels or the k -modes model. The zoo data achieved a maximum ARI of 0.88 at $K = 5$, a strong indication of clustering, but below the reported value of $K_t = 7$. Thus there may be insufficient information to distinguish all seven reported clusters, but the labels appear to be consistent with the detectable structure in the zoo data.

2) *Simulation*: We undertook a simulation study to explore the behavior of the proposed OTQT and OT algorithms and the existing H97 k -modes algorithm, the initialization methods, and the K -selection methods. We simulated 20 replicate samples of size $n = 1000$ with 4 categories possible at each of $p \in \{5, 10\}$ coordinates, $K \in \{2, 5\}$ clusters, and four levels of clustering difficulty (Figure 2 (b)).

We allow unequal-sized clusters by simulating the cluster proportions as $\pi \sim \text{Dirichlet}(1, 1, \dots, 1)$. Then, the cluster sizes $(|C_1|, |C_2|, \dots, |C_K|)$ follow a Multinomial(1000, π) distribution. To guarantee K clusters, we discard any simulation with $|C_k| = 0$ for any $1 \leq k \leq K$. To simulate the observations, we assume a nested continuous time Markov chain (CTMC) model. This model is flexible, but we use a particularly simple formulation, where the rate of change between categories is equal. In this case, choosing realization times is equivalent to choosing a probability of change, and conditional on change, all substitutions are equally likely. In the inner level, we simulate K modes from an “ancestor” observation. The ancestor is generated with independent coordinates and uniform category probabilities. Then, each coordinate of each mode is sampled by initializing an independent realization of the CTMC from the corresponding ancestor state. In our simulations, the inner CTMC

³This breast cancer domain was obtained from the University Medical Centre, Institute of Oncology, Ljubljana, Yugoslavia. Thanks go to M. Zwitter and M. Soklic for providing the data.

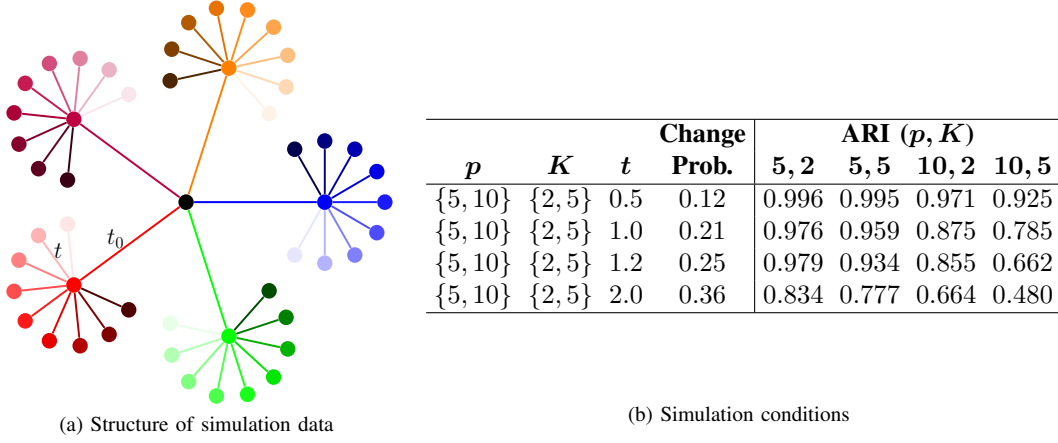


Fig. 2. Simulations. (a) Nested simulation structure models K (here, 5) modes as independent realizations of a CTMC initialized with the center, black observation and evolved for time t_0 . The observations are then simulated as independent realizations of a second CTMC initialized from each mode and evolved for time t . Better separation of clusters, and easier data to cluster, are produced as t_0/t increases. (b) p is the number of coordinates, K is the true number of clusters, and t is the aforementioned indication of clustering difficulty (t_0 is held constant). For each t , there is an induced Change Prob., the expected proportion of changed coordinates in an observation, relative to the mode. We also report the median, among the 20 replicates, of mean adjusted Rand index [34] at the true K (see Methods).

results in a 70% chance of change at each coordinate. To guarantee K distinct modes, we discard any simulation with two or more identical modes. Finally, we simulate the $|C_k|$ independent observations within cluster k by applying independent CTMC realizations to each coordinate for t time units. In our simulations, we explore four values of $t \in \{0.5, 1, 1.2, 2\}$, resulting in probabilities of change that vary from 12% to 36% (Figure 2 (b), “Change Prob.”). These simulation conditions produce data with varying difficulty of clustering. To illustrate, we report the median of mean ARIs [34]. Specifically, for each simulated datasets, we compute the mean ARI observed for solutions achieving the smallest observed criterion (3) at the true K . The median across the 20 simulated datasets is reported in Figure 2 (b). Clustering difficulty increases with t , K , and p .

3) *Analysis Methodology*: We analyze both real and simulated datasets by initializing each of the three algorithms (H97, OTQT, and OT) with each initialization method (**klar**, **py**, **h97r**, **clbr**, and **km++** and non-updating variants) $\alpha n K p'$ times. Specifically, for each initialization method, all three algorithms are initialized with the same $\alpha n K p'$ initializations. This experimental structure creates dependence between the algorithm results, which is accommodated throughout the analyses that follow. K ranges in $\{1, 2, \dots, 2K_t + 1\}$ for the real datasets (except mushroom, where the upper limit is $2K_t + 2$, because of a local peak in the ARI at $K = 4$, Fig. 1) and $\{1, 2, \dots, 2K_t - 1\}$ for the simulated datasets with $K_t = 5$ and $\{1, 2, \dots, 2K_t\}$ for the simulated datasets with $K_t = 2$, where K_t is the reported or true number of clusters. The multiplier α and thus the number of runs (independent initializations) is chosen to be the smallest integer multiple such that $\alpha n p' \max\{K\}$ exceeds 500,000. For the real data, n and p' are the data dimensions as reported in Table I. For simulation, $n = 1,000$, $p' \in \{5, 10\}$, and $K_t \in \{2, 5\}$ as reported in Figure 2 (b). Since $p' = p$ for the simulated data, we may interchangeably use p and p' when discussing simulation data.

We compare the algorithms and initialization methods in terms of both accuracy per initialization and time to reach a target value of objective function (3). Ideally, the target value is the global minimum, but this value is unknown, even for the simulated data. For the real data, we assume the minimum achieved across all algorithms and initialization methods is the global minimum. This target is achieved frequently enough to perform statistical tests, except in the splice dataset. In this case and for all simulation datasets, we consider the target met if the minimum is at or below the 5th percentile achieved across all initialization methods and algorithms. Henceforth, we refer to this value of the objective function as the “target”.

To compare the accuracies of pairs of algorithms, we count the number of initializations that achieve the target. Given an initialization method and a pair of algorithms to compare, we count the number of times the first algorithm achieves the target and the second does not (n_{10}) and vice versa (n_{01}). If there is no difference between algorithms, then conditional on $N_{10} + N_{01} = n_{10} + n_{01}$, $N_{10} \sim \text{Bin}(n_{10} + n_{01}, 0.5)$. To avoid the situation where $n_{10} + n_{01} = 0$, we approximate this distribution as $\text{Bin}(n_{10} + n_{01} + 2, 0.5)$ and assess the left tail probability as $\Pr(N_{10} \leq n_{10} + 1)$. Discrepancy between the true distribution and this approximation will be highest for low counts and consequently, less significant test results. To retain the precision of extreme tail probabilities both near 0 and near 1, when $n_{10} > n_{01}$, we instead compute $\Pr(N_{01} \leq n_{01}) = 1 - \Pr(N_{10} \leq n_{10} + 1)$. We use Holm’s method [37] to correct the probabilities for multiple testing, then cap the resulting values at 0.5 (Holm’s method caps them at 1). Finally, we negate the values with $n_{10} > n_{01}$ and apply a probit-like transformation $-\text{sign}(x)\Phi^{-1}(|x|)$ to map the values to the real line, such that data supporting the superiority of the first algorithm approach ∞ , while data supporting the superiority of the second algorithm approach $-\infty$. To quantify the effect size, we compute confidence intervals for rate

ratio $r = \frac{n_{10}+1}{n_{01}+1}$ using

$$\left(r \exp \left[-q_{0.975} \sqrt{\frac{1}{n_{10}+1} + \frac{1}{n_{01}+1}} \right], r \exp \left[q_{0.975} \sqrt{\frac{1}{n_{10}+1} + \frac{1}{n_{01}+1}} \right] \right),$$

where $q_{0.975}$ is the $(1 - \alpha/2)$ quantile of the standard normal distribution with $\alpha = 0.05$.

To compare the accuracies of pairs of initialization methods, we also count the number of initializations that achieve the target. This time, the initializations are independent, so we merely count the number n_1 of initializations that reach the target using the first initialization method, and the number n_2 that reach the target using the second initialization method. Then, conditional on $N_1 + N_2 = n_1 + n_2$, $N_1 \sim \text{Bin}(n_1 + n_2, 0.5)$, with no concern for 0 counts. The rest of the analysis is as for the paired algorithms.

To compare the speed of the methods, we record the real time in seconds, also known as “wait times”, between initializations that strike the target. To compare algorithms, if the first algorithm strikes the target with a wait time of T_1 and the second algorithm strikes the target with a wait time of T_2 , then we perform a Wald’s test of equal mean wait times, $\mathbb{E}[T_1] = \mathbb{E}[T_2]$, using statistic $(\bar{T}_1 - \bar{T}_2) / \sqrt{\text{Var}(\bar{T}_1 - \bar{T}_2)}$, where $\text{Var}(\bar{T}_1 - \bar{T}_2) = \text{Var}(T_1)/n_1 + \text{Var}(T_2)/n_2 - \frac{2}{n_1 n_2} \sum_{i=1}^{n_1} \sum_{j=1}^{n_2} \text{Cov}(T_{1i}, T_{2j})$, T_{1i} is the i th of n_1 observed wait times for method 1 and T_{2j} the j th of n_2 observed wait times for method 2. The variances are estimated from the sample variance of the observed wait times. For the covariance, we assume that pairs of initializations are independent and identically distributed, and therefore the covariance between any two wait times is determined by the number of initializations they share in common, so

$$\text{Cov}(T_{1i}, T_{2j}) = c_{12} \mathbb{1}\{\min\{r_{i1}, r_{j2}\} > \max\{l_{i1}, l_{j2}\}\} (\min\{r_{i1}, r_{j2}\} - \max\{l_{i1}, l_{j2}\}),$$

where c_{12} is the estimated covariance of the paired times to complete one initialization, estimated from the $\alpha n p' K$ initializations, l_{il} and l_{jl} are the indices of the previous initialization to hit the target (or 0 if none), and r_{il} , r_{jl} are the indices of the i th and j th strike on the target for $l \in \{1, 2\}$ indicating the method. Confidence intervals for time to target ratio \bar{T}_1/\bar{T}_2 are computed via Fieller’s method [38]. The analysis to compare initialization methods for their time to target is identical except all initializations are independent and the covariance is $c_{12} = 0$.

We test for equal accuracy $\Pr(\hat{K}_t = K_t)$ when comparing K_t -estimation methods using Wald’s tests and accounting for covariation between K estimates obtained from identical datasets. Originally, we run simulation data for all $K \in \{1, 2, \dots, 2K_t - 1\}$ for $K_t = 5$ and $K \in \{1, 2, \dots, 2K_t\}$ for $K_t = 2$. Jump statistics can choose \hat{K}_t to be any of these values, but the KL statistics cannot choose \hat{K}_t to be the boundary values. Thus, we constrain all K -selection methods to estimate $\hat{K}_t \in \{2, 3, \dots, 2K_t - 2\}$ for $K_t = 5$ simulations, and $\hat{K}_t \in \{2, 3\}$ for $K_t = 2$ simulations. Note, the DM statistic can also not estimate $\hat{K}_t = 1$, since the optimum for $K = 1$ is deterministic and there are no wait times to the target optimum to measure.

B. Results

1) *Real-World Data:* The proposed OTQT and OT algorithms are almost universally more accurate than the H97 algorithm (that of [15]) as measured by the proportion of initializations achieving a target minimum of the objective function (3). To formally compare pairs of algorithms in the context of a given initialization method, we run them on the same initializations and count the number of runs where the first algorithm achieves the target minimum but the second does not (n_{10}) and vice versa (n_{01}). In Table II, we report the range of rate ratios $(n_{01} + 1)/(n_{10} + 1)$ for H97 against OT at the true K_t across initialization methods; Fig. 3 (a) shows details (note, the ratio is inverted in Table II). We also examine the left tail probabilities $\Pr(N_{10} \leq n_{10})$, which are close to 1 if the first algorithm is superior to the second or near 0 if the second algorithm is superior. Controlling the family-wise error rate (FWER) at 0.05 [37], a null hypothesis of equal accuracy is strongly rejected in nearly all cases, and only the breast cancer dataset at $K = 2$ found H97 significantly better than OTQT (Fig. 3a). OTQT and OT were less likely to differ and if they did, the effect size was smaller. For the senators and soybean datasets, OTQT was superior to OT for intermediate values of K , while on the splice dataset, OT had a tiny, but significant, advantage over OTQT (Fig. 9).

The algorithmic efficiency of H97 does not make up for fewer initializations arriving at the target; it takes more average time to achieve the target than either the OTQT and OT algorithms. To compare times, we collect data on the time until convergence of each run, including initialization but excluding bookkeeping (e.g., for computing ARI). We report average cumulative run time to achieve the target minimum for each algorithm using repeated initializations with method **klar** at the true K_t in Table II; more initialization methods and details are in Fig. 3 (b). OT is the fastest to the target minimum on all but the mushroom dataset, where OTQT is faster (Table II), but OTQT is faster than H97 on all but the splice dataset (Fig. 3 (b)). H97 is also a fraction faster than OTQT on the breast cancer and soybean datasets for specific choices of K . The speed advantage of the OT-containing algorithms increases with K , especially for K larger than the true K_t . OT is usually significantly faster than OTQT, but they differ less than either differs from H97 (Fig. 9 (b)).

We can find little difference in the ability of the initialization methods to achieve better minima on the real data. To compare initialization methods, we count the number of times, n_1 and n_2 , that the two initialization methods achieve the target minimum. Controlling FWER at 0.05, there are no significant differences in the accuracies of the initialization methods except between

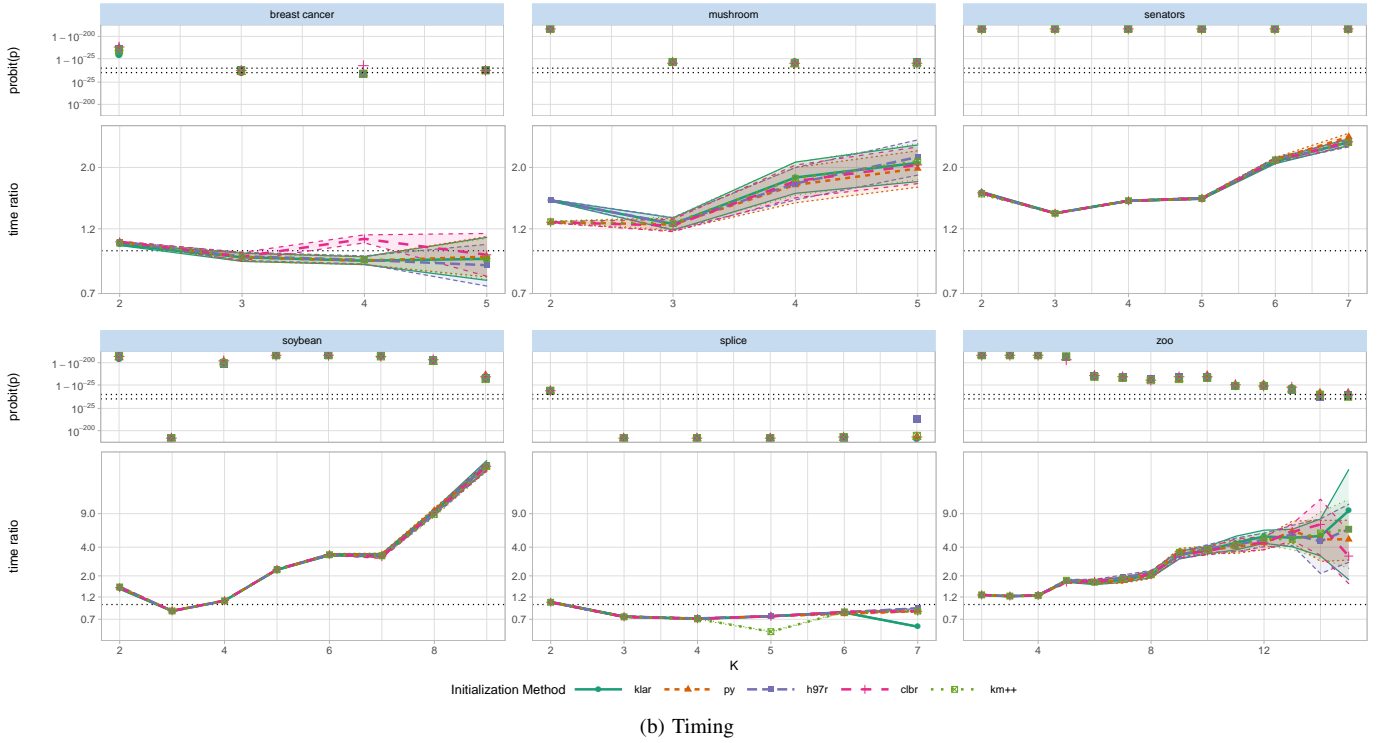
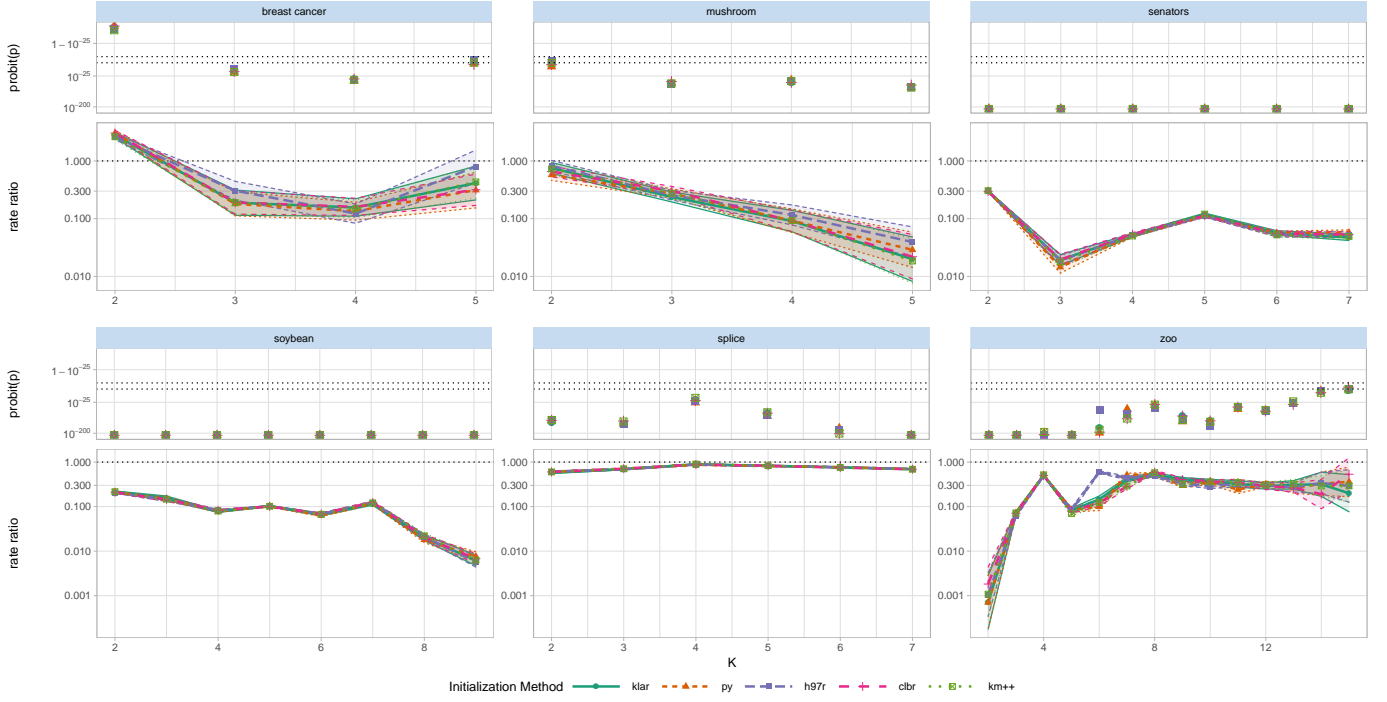


Fig. 3. Comparison of H97 and OTQT on real datasets. In the 12 pairs of plots, the top has the probit-transformed, adjusted left tail probabilities for the tests of (a) equal initializations or (b) equal real time to reach the target minimum for both algorithms. The horizontal dotted lines delimit the region where the null hypothesis cannot be rejected when controlling FWER at 0.05. The bottom plots show the rate ratios (a) or time ratios (b) with 95% confidence intervals on the log10 scale, with no difference marked by the horizontal dotted line. Colors and symbols indicate the initialization method. The y -axes are linked across facets in a row; the x -axes are not linked across plots nor identically labeled.

TABLE II

RESULTS ON REAL DATA. TO COMPARE THE ALGORITHMS AT THE TRUE K_t , WE REPORT THE RANGE OF RATIOS ACROSS INITIALIZATION METHODS OF THE NUMBER OF INITIALIZATIONS ACHIEVING THE GLOBAL MINIMUM FOR OTQT OVER H97 (BOLDED IF p -VALUE $< 1 \times 10^{-3}$). THE AVERAGE TIME, IN SECONDS, TO ACHIEVE THE GLOBAL MINIMUM AT THE TRUE K_t , USING RANDOM INITIALIZATION (**klar**), IS REPORTED FOR ALGORITHMS H97, OTQT, AND OT. WE PRESENT ESTIMATED K USING TEN DIFFERENT METHODS: BOLDED VALUES MATCH EITHER THE TRUE K_t (TABLE I) OR THE K WITH MAXIMUM ARI (FIG. 1), ITALICIZED NUMBERS ARE ONE ABOVE OR BELOW THESE VALUES, NA INDICATES THE STATISTIC SUPPORTING THIS K COULD NOT BE SIGNIFICANTLY DISTINGUISHED FROM 0. [†]THE SPLICE DATA DID NOT REPEATEDLY ACHIEVE THE MINIMUM VALUE OF THE OBJECTIVE FUNCTION, SO ALL VALUES ARE COMPUTED FOR MINIMA AT OR BELOW 5TH QUANTILE OF ALL ACHIEVED MINIMA.

Data	OTQT/H97		Avg. time to min. (s)				K_{\min} , K_{\max}	Estimated K									
	min	max	H97	OTQT	OT	Scale		\hat{K}_J	\hat{K}_{iJ}	\hat{K}_{hJ}	\hat{K}_{Jt}	\hat{K}_{iJt}	\hat{K}_{hJt}	\hat{K}_{KL}	\hat{K}_{iKL}	\hat{K}_{hKL}	\hat{K}_{DM}
c	0.33	0.38	3.0	2.8	2.7	10^{-4}	[2, 4]	2	2	4	2	2	4	3	3	2	3
m	1.21	1.75	12	7.7	7.8	10^{-2}	[2, 6]	6	6	6	6	6	6	5	3	3	4
se	51.6	69.9	1.4	1.0	1.0	10^{-3}	[2, 6]	6	6	6	NA	NA	NA	3	4	3	6
so	12.1	12.9	1.3	1.1	1.1	10^{-4}	[2, 8]	8	7	8	3	NA	3	3	3	3	4
sp [†]	1.41	1.45	2.2	3.0	2.1	10^{-1}	[2, 7]	4	4	5	4	4	5	4	2	3	4
z	1.95	3.51	16	8.7	8.2	10^{-2}	[2, 14]	14	13	13	2	NA	2	4	8	10	4

methods that do and do not update modes during the first iteration. (We will thoroughly discuss this phenomena when analyzing the simulation results, where the patterns are similar.) There are significant differences in the mean times to the target minimum, but because the counts n_1 and n_2 do not differ, the cause must be varying algorithmic costs of initialization. Specifically, there are 159 out of 1,320 significant results while controlling FWER at 0.05 when comparing mean time to the target minimum, however there is no consistently better initialization method across estimation K , and especially not across datasets. We find the differences between initialization methods are better resolved on the simulation data to be discussed later.

We try ten different methods to estimate K . No single method works reliably on all real datasets to obtain the reported “true” K_t or the K with maximal ARI (Table I). Most methods tend to overestimate K , but underestimation is also possible. One troubling observation is the tendency for the jump statistic to not only overestimate K , but to choose the maximum considered K . This trend continues even after increasing K further (data not shown). The weighted and bootstrapped jump variants are less likely to severely overestimate K , but are still susceptible to the problem. Overall, the KL methods choose more reasonable K than the jump methods, with the novel DM method somewhere in between. We also observe KL and DM methods to produce more stable estimates of K across multiple runs (data not shown). [32] indicate that the power y used in the jump statistic needs to be adjusted for non-Gaussian, non-independent coordinates. Our strategy of using $y = p'$ (see §II) accounts for the non-independence of coordinates, but it is unclear how the y should be further adjusted for the categorical distributions used in k -modes. Finally, it is completely plausible that the real datasets examined in this study do not satisfy the assumptions of the k -modes model.

2) *Simulation Data*: Because we replicate each simulation condition 20 times, it is possible to show trends across features of the data, such as dimension (p), number of clusters (K_t), and difficulty of clustering (t). Whereas in real data we compare methods across initializations, for simulation data, we compare methods across replicates.

Just as for the real data, the OTQT algorithm is significantly more accurate than the H97 algorithm as measured by the proportion of initializations achieving the target value of the objective function (Fig. 4(a) for $K_t = 5$, Fig. 10(a) for $K_t = 2$). We plot the significance (transformed left tail probabilities, upper plots in each pair) and magnitude (log10 rate ratios, lower plots) of the difference in the targeting rates for the two algorithms. The OTQT algorithm is significantly more likely to achieve the target minimum than H97, except perhaps when true $K_t = 5$ and estimation $K = 2$. The benefit of the OTQT algorithm increases with estimation K and the difficulty of clustering (increasing t). When $K_t = 5$ and clusters are well separated ($t = 0.5$) the difference between H97 and OTQT peaks near $K = K_t$, but the phenomena is not universal, and thus not generally useful for detecting the true K .

OTQT is usually faster than H97 (Fig. 4(b)). As for the real data, the speed of H97 can make up the accuracy difference so that it achieves the target slightly faster than OTQT under select conditions. At $K_t = 5$, $p = 5$, $t = 2$, and $K > 4$, there is a small temporal advantage of H97 per initialization (average 0.11ms; interquartile range -0.16 – 0.39ms), with H97 significantly better than OTQT in 60% of the simulations. In contrast, the accuracy advantage of OTQT at $p = 10$ does translate into a speed advantage over H97 (average 11ms; interquartile range 0.14 – 8.9ms; significantly better in 87% of simulations) that increases with K so that by $K = 9$, 100% of the differences are significant (average 44ms; interquartile range 11 – 55ms). For the simulation with $K_t = 2$, OTQT is faster than H97 except for $K = 2$ and good separation ($t = 0.5$), although the advantage of OTQT is often not significant at $K = 3$ (Fig. 10(b)). Overall, there appears to be little cost to using OTQT and almost always an advantage.

a) *Initialization methods*:: In contrast to the real data results, we find differences between the initialization methods with the increased power of the simulation design. We examine the initialization methods in two ways. In the first, we rank the initialization methods from best to worst on each dataset (Fig. 5, Table III, and Fig. 13 for $K_t = 5$, Fig. 14 for $K_t = 2$). In the second, we mimic the pairwise comparison of the H97 and OTQT algorithms, plotting the significance and magnitude of the difference between pairs of initialization methods (Fig. 15 for $K_t = 5$, Fig. 16 for $K_t = 2$).

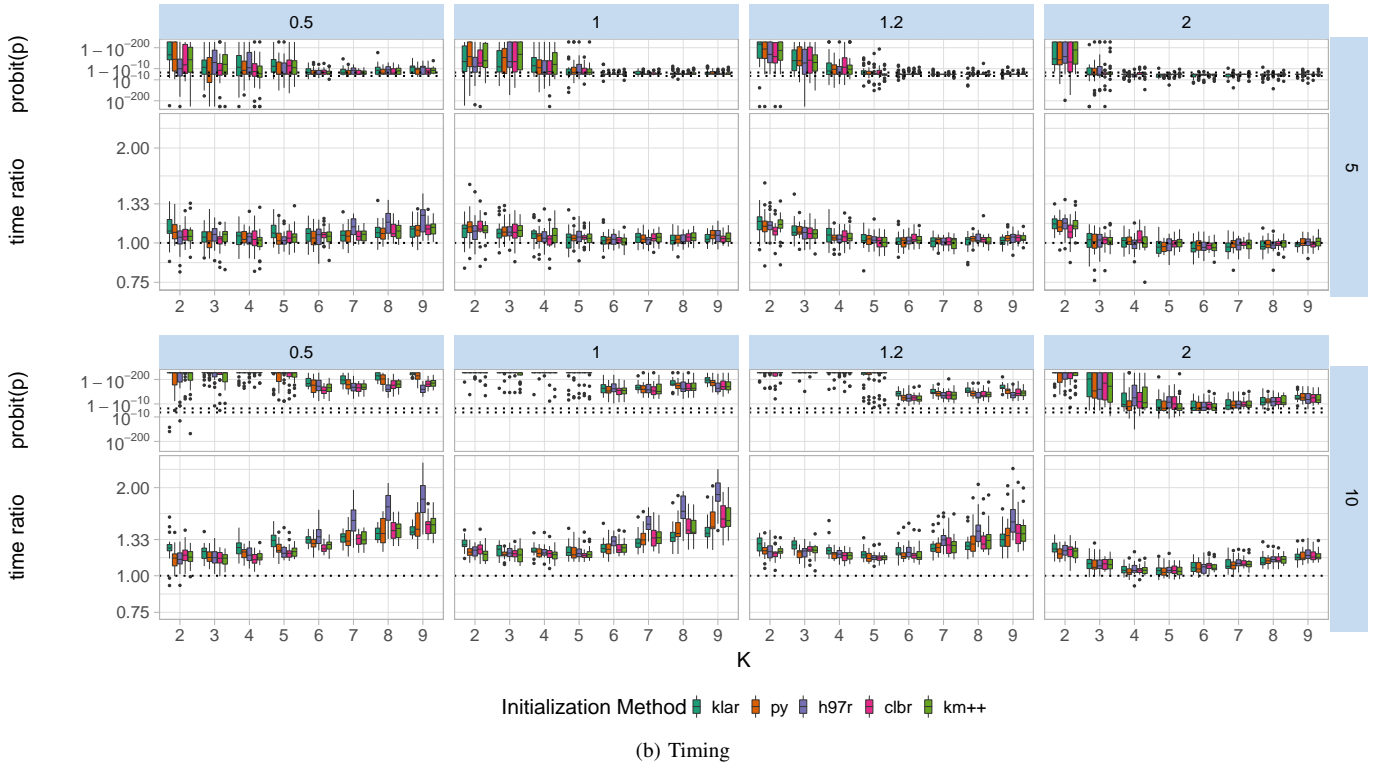
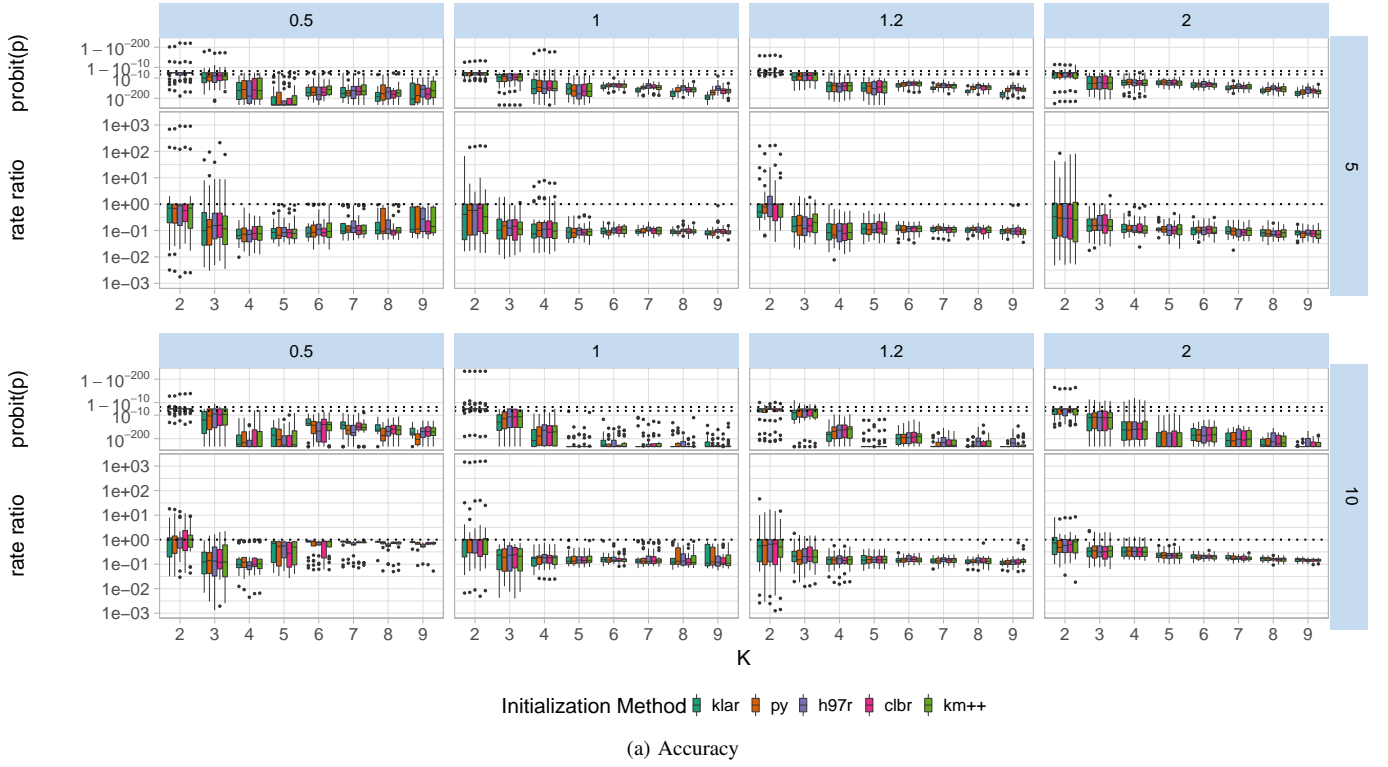


Fig. 4. Accuracy and timing of H97 vs. OTQT at $K_t = 5$. In each pair of plots, we use boxplots to summarize the probit-transformed, adjusted left-tail probabilities (upper plots) and log10-transformed ratios (lower plots) at each K (horizontal position) for each initialization method (color). The dotted horizontal lines in the upper plots demarcate the acceptance region for the null hypothesis of no change when FWER is 0.05. The dotted horizontal line in the bottom plots indicate no difference between the H97 and OTQT algorithms.

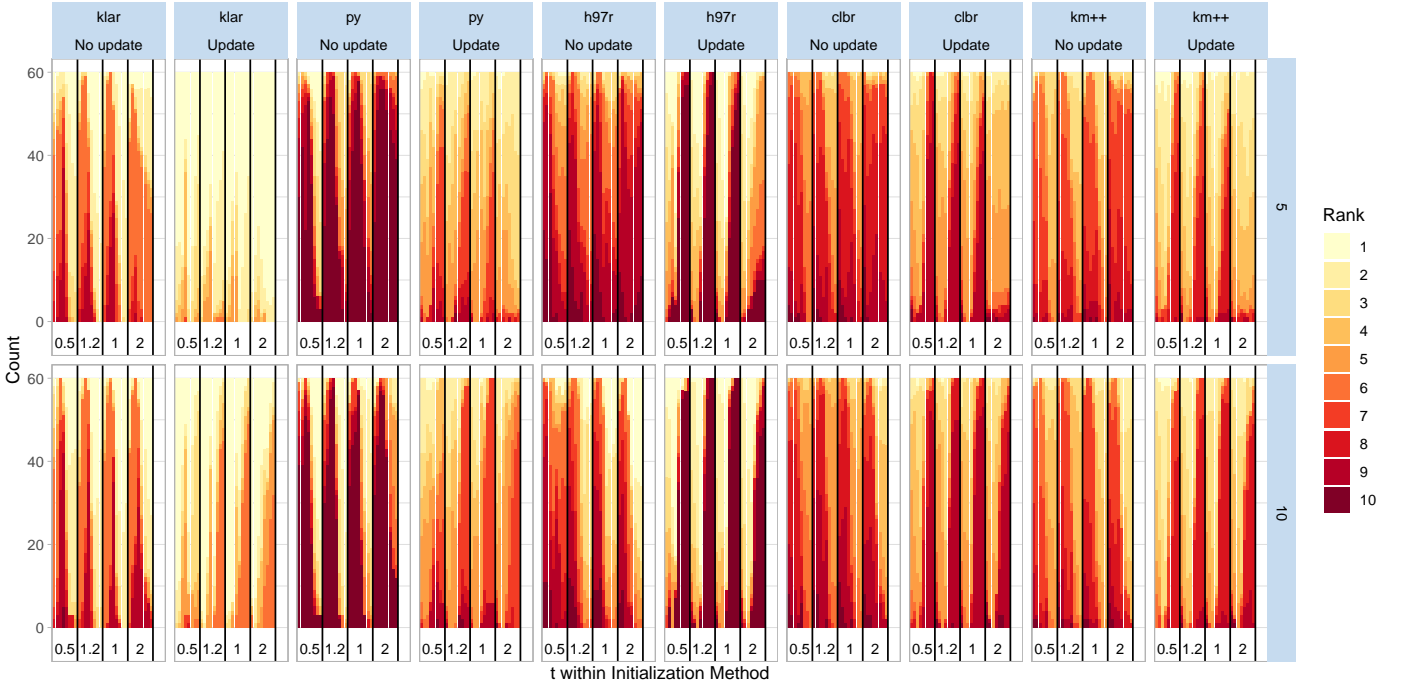


Fig. 5. Ranks of five initialization methods based on time to achieve target minimum with algorithm H97 on simulated data $K_t = 5$. Each facet is a different pair of simulation p and initialization method (**klar**, **py**, **h97r**, **clbr**, **km++**, with and without updates), and each block shows the achieved ranks at the indicated simulation difficulty t among the 20 replicates at $K \in \{2, 3, \dots, 9\}$. If a column is entirely light yellow, such as **klar** with updates for $p = 5$, $t = 2$, and small K , then the indicated initialization method beats all other initialization methods in all 20 replicates.

TABLE III

AVERAGE RANK OF INITIALIZATION METHODS. MEAN AND STANDARD DEVIATION OF RANK PERFORMANCE OF EACH INITIALIZATION METHOD FOR RUNS ON ALL SIMULATIONS, RUNS SELECTING $K \leq K_t$, AND RUNS SELECTING $K > K_t$. THE TOP BLOCK RANKS METHODS BASED ON NUMBER OF INITIALIZATIONS ACHIEVING THE TARGET; THE BOTTOM BLOCK RANKS METHOD BY REAL TIME TO ACHIEVE THE TARGET. THE BEST PERFORMER (LOWEST RANK) IS SHOWN IN BOLD IN EACH CASE.

	With Update					Without Update				
	klar	py	h97r	clbr	km++	klarn	pyn	h97rn	clbrn	km++n
All	5.7 (1.7)	5.9 (2.2)	7.5 (3.9)	6.6 (3.0)	6.3 (2.9)	6.6 (3.4)	6.9 (3.8)	6.2 (2.9)	6.6 (1.9)	6.6 (2.0)
$\leq K_t$	5.7 (1.4)	4.5 (1.6)	4.1 (2.8)	4.1 (1.8)	3.8 (1.8)	9.4 (2.4)	9.5 (2.4)	8.1 (2.0)	7.9 (1.4)	7.9 (1.4)
$> K_t$	5.8 (1.9)	7.2 (1.8)	10.3 (1.8)	8.7 (2.0)	8.3 (2.0)	4.2 (2.2)	4.7 (3.4)	4.6 (2.6)	5.5 (1.6)	5.5 (1.7)
All	2.5 (2.0)	5.4 (2.3)	6.8 (4.1)	6.7 (2.9)	5.7 (2.8)	4.3 (3.0)	7.5 (3.7)	6.9 (2.9)	7.3 (2.0)	6.4 (2.1)
$\leq K_t$	1.8 (1.4)	3.9 (1.5)	3.0 (2.2)	4.4 (1.6)	3.5 (1.6)	6.5 (1.8)	9.9 (1.8)	8.5 (1.7)	8.4 (1.3)	7.7 (1.3)
$> K_t$	3.1 (2.3)	6.6 (2.2)	9.9 (2.3)	8.6 (2.2)	7.5 (2.4)	2.5 (2.1)	5.5 (3.6)	5.6 (3.0)	6.3 (.20)	5.3 (2.0)

For both analyses, we compare initialization methods in terms of accuracy (Fig. 13 for $K_t = 5$) and real time (Fig. 5 for $K_t = 5$) to the target minimum (both in Fig. 14 for $K_t = 2$). Overall, initializing with random modes, **klar** initialization, achieves the target faster than any other initialization method (Fig. 5 and Table III). **Klar** is not necessarily more accurate (Table III); other methods clearly dominate it under specific simulation conditions (Fig. 13). Thus, **Klar** is faster not because it is accurate, but because it is computationally cheap. The other patterns observed in accuracy and timing are similar. As seen for the real data, the biggest contrast is seen between initialization methods that update modes during the first iteration (**klar**, **py**, **h97r**, **clbr**, and **km++**) vs. those that do not (**klarn**, **pyn**, **clbrn**, and **km++n**). Adding updates can benefit a method (**klar** or **py**) or hurt a method (**clbr** or **h97r**, especially see Fig. 14), but the most obvious effect is an interaction with the number of clusters K . The contrast between performances for $K < K_t$ vs. $K > K_t$ is striking: almost any method that dominates in accuracy for small K fails for large K and vice versa. Updates help when $K < K_t$ and no updates help when $K > K_t$. Other than this major pattern, performance differences are enhanced with high overlap $t = 2$ and methods **py** and **h97r** are particularly sensitive to update and t effects. The patterns are similar for $K_t = 2$ (Fig. 14(a) and 16(b)), and for algorithms OTQT and OT (data not shown).

b) *Choosing K* : We test ten different methods for selecting K (Fig. 6 and Table IV). For a fair comparison, we restrict all methods to select $\hat{K}_t \in \{2, 3\}$ for $K_t = 2$ and $\hat{K}_t \in \{2, 3, \dots, 8\}$ for $K_t = 5$, even though the jump statistic may select $\hat{K}_t = 1$, and both the jump statistics and the DM statistic can select one additional integer at the upper limit. Among existing methods and in contrast to the behavior in real data, the jump statistics tend to select $\hat{K}_t < K_t$. Weighting by the inverse

mean reduces and reverses this trend for the i^* variants, but at the cost of accuracy and precision at $K_t = 2$. Bootstrapping has either little effect or reduces performance for $p = 10$ with both weighting schemes (iJ_t and hJ_t). The KL statistic does well for $K_t = 2$, where the choices for \hat{K}_t are highly constrained, but fails to retain the strength at $K_t = 5$. The iKL variant is the best among KL methods, but is dominated by iJ at $K_t = 5$.

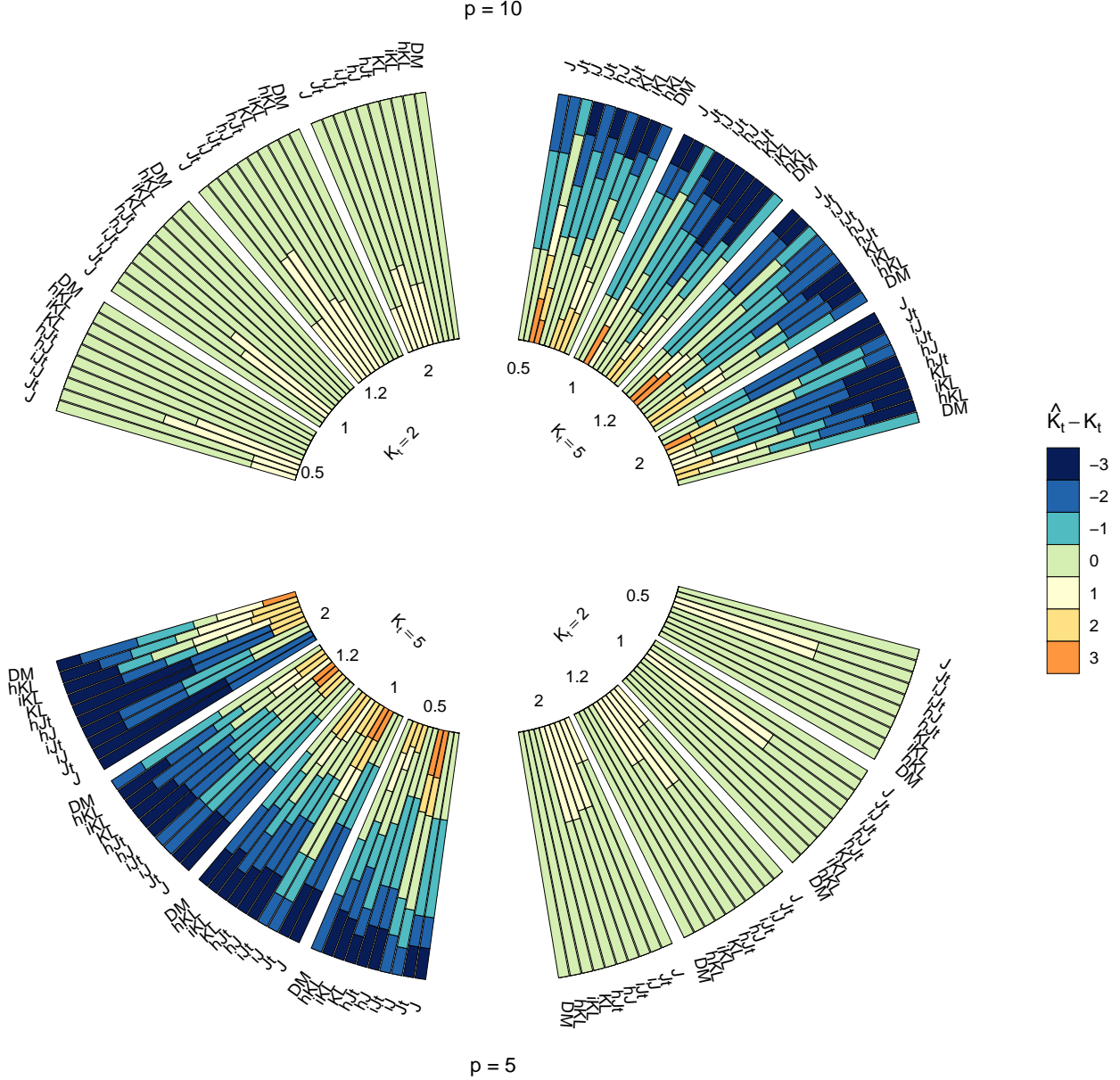


Fig. 6. Estimated \hat{K}_t by ten methods. The proportion, out of the 20 simulated datasets, selecting the K_t with the specified error. Each quadrant corresponds to a distinct choice of p and K_t ; each block corresponds to a choice of t .

To better assess the ability of the methods to find real structure in the datasets, we examine the ARI distributions at the selected \hat{K}_t s (Fig. 7). Among the jump statistics, J and J_t are effectively equivalent, but they give both strong and weak performances depending on the simulation conditions. Weighted variants iJ and hJ_t also have a distinctive and similar performance, sometimes performing better ($K_t = 5$), but also worse ($K_t = 2$) depending on the simulation conditions. The weighted hKL gives almost universally worse performance, whereas iKL can improve performance for $K_t = 2$, but not $K_t = 5$. Overall it is discouraging that among the K selection methods adapted from k -means to k -modes, there is no universal winner; it is difficult to make a single recommendation.

We discovered the tenth K selection method when implementing our k -modes initialization methods. The k -modes algorithms proposed by [15] and [14] differ in whether they update the mode immediately after a change in cluster membership. This distinction is also true during the first iteration as observations are added to the clusters, although not all readers have interpreted the initial iteration the same way [39]. For the record, Hartigan and Wong’s k -means also postpones updates until the first iteration is complete [11]. We have already noted the very strong impact of including updates during the first iteration (*e.g.*,

TABLE IV

ACCURACY AND PRECISION OF SELECTED \hat{K}_t BY TEN METHODS. THE PROPORTION OF CORRECT $\hat{K}_t = K_t$ (ACCURACY; LEFT) AND THE MEAN SQUARED ERROR (MSE; RIGHT). BOLDED NUMBERS ON THE LEFT ARE THE HIGHEST PROPORTIONS; BOLDED NUMBERS ON THE RIGHT ARE THE LOWEST MSEs IN EACH ROW. SIGNIFICANT p -VALUES BASED ON A WALD TEST COMPARING THE MOST BOLDED METHOD AGAINST OTHERS ARE FOOTNOTED.

Simulation				K_t Estimation Method											
K_t	p	t		J	Jt	iJ	iJ _t	hJ	hJ _t	KL	iKL	hKL	DM		
Accuracy: $\Pr\left(\hat{K}_t = K_t\right)$	2	5	0.5	1.00	1.00	0.30 ^d	0.30 ^d	1.00	0.95	1.00	1.00	1.00	1.00		
			1	1.00	1.00	0.30 ^d	0.30 ^d	1.00	1.00	1.00	1.00	1.00	1.00		
			1.2	0.95	0.95	0.60 ^b	0.60 ^b	0.85	0.85	1.00	1.00	1.00	1.00		
		10	2	0.95	0.95	0.75	0.75	0.70 ^a	0.70 ^a	1.00	1.00	1.00	1.00		
			0.5	0.95	0.95	0.35 ^d	0.45	1.00	0.80	1.00	1.00	1.00	1.00		
			1	1.00	1.00	0.65 ^a	0.35	1.00	0.85	1.00	1.00	1.00	1.00		
	5	10	1.2	0.85	0.85	0.35 ^d	0.30 ^b	0.80	0.75	1.00	1.00	1.00	1.00		
			2	0.95	0.95	0.80	0.75	0.90	0.90	1.00	1.00	1.00	1.00		
			0.5	0.40	0.40	0.60	0.55	0.30	0.30	0.35	0.40	0.10	0.70		
		5	1	0.20	0.20	0.40	0.40	0.20	0.20	0.15	0.20	0.20	0.40		
			1.2	0.15	0.15	0.50	0.50	0.20	0.20	0.10	0.25	0.10	0.60		
			2	0.00	0.00	0.25	0.25	0.00	0.00	0.10	0.15	0.05	0.05		
	10	5	0.5	0.40	0.40	0.40	0.25	0.55	0.50	0.40	0.40	0.40	0.70		
			1	0.25 ^b	0.25 ^b	0.65	0.40	0.30	0.30	0.10 ^a	0.40	0.05	0.80		
			1.2	0.20 ^b	0.20 ^b	0.80	0.40	0.30 ^a	0.30 ^a	0.15 ^a	0.40	0.15	0.85		
		10	2	0.10 ^a	0.10 ^a	0.55	0.60	0.15	0.15	0.00	0.15	0.10	0.60		
			Overall			0.58 ^b	0.58 ^b	0.52 ^d	0.45 ^d	0.58 ^b	0.55 ^b	0.58 ^a	0.65	0.57 ^a	0.79
			Mean Squared Error: $\mathbb{E}\left[\left(\hat{K}_t - K_t\right)^2\right]$	2	5	0.5	0.00	0.00	0.70 ^d	0.70 ^d	0.00	0.20	0.00	0.00	0.00
1	0.00	0.00				0.70 ^d	0.70 ^d	0.00	0.00	0.00	0.00	0.00	0.00		
1.2	0.05	0.05				0.40 ^b	0.40 ^b	0.15	0.15	0.00	0.00	0.00	0.00		
10	2	0.05			0.05	0.25	0.25	0.30 ^a	0.30 ^a	0.00	0.00	0.00	0.00		
	0.5	0.05			0.05	0.65 ^d	1.30 ^d	0.00	0.80 ^c	0.00	0.00	0.00	0.00		
	1	0.00			0.00	0.35 ^a	1.55 ^d	0.00	0.60 ^b	0.00	0.00	0.00	0.00		
5	10	1.2		0.15	0.15	0.65 ^d	1.00 ^d	0.20	0.55 ^a	0.00	0.00	0.00	0.00		
		2		0.05	0.05	0.20	0.40 ^a	0.10	0.10	0.00	0.00	0.00	0.00		
		0.5		1.15	1.15	2.05 ^b	2.25 ^c	1.80 ^d	1.80 ^d	1.35	2.70 ^d	3.10 ^d	0.75		
	5	1		3.30 ^c	3.30 ^c	2.00	2.00	3.60 ^c	3.60 ^c	2.80	2.95	3.75 ^b	2.00		
		1.2		3.75 ^d	3.75 ^d	1.25 ^a	1.25 ^a	3.95 ^d	3.95 ^d	3.70 ^d	2.75 ^d	4.50 ^d	0.55		
		2		7.50 ^d	7.50 ^d	2.45	2.45	7.25 ^d	7.25 ^d	4.20 ^a	3.45	3.05	3.05		
10	5	0.5		1.05 ^a	1.05 ^a	2.25 ^d	3.00 ^d	0.75	1.20 ^a	1.05 ^a	2.25 ^d	2.00 ^c	0.45		
		1		1.30 ^d	1.30 ^d	1.15 ^c	1.15 ^d	1.80 ^d	1.80 ^d	4.95 ^d	2.80 ^d	4.20 ^d	0.20		
		1.2		2.10 ^d	2.10 ^d	0.60	2.25 ^d	1.30 ^d	1.30 ^d	2.80 ^d	2.45 ^d	3.45 ^d	0.30		
	10	2		4.50 ^d	4.50 ^d	1.15 ^a	0.70	4.05 ^d	4.05 ^d	4.80 ^d	3.25 ^d	3.65 ^d	0.40		
		Overall			1.56 ^d	1.56 ^d	1.05 ^d	1.33 ^d	1.58 ^d	1.73 ^d	1.60 ^d	1.41 ^d	1.73 ^d	0.48	

^a $p < 0.01$ ^b $p < 10^{-3}$ ^c $p < 10^{-4}$ ^d $p < 10^{-5}$

Fig. 5). The interaction with K suggest that timing information could reveal the true K_t . As shown in Fig. 8, the clearest signal comes by contrasting the updated and non-updated initializers. The DM K -selection method, which set \hat{K}_t to the choice of K minimizing the timing ratio $\bar{T}_{\text{klar}}/\bar{T}_{\text{klam}}$ is more accurate than the other K selection methods (Table IV). Not only does this method more often select the true K_t , the solutions have consistently higher ARI (Fig. 7 for $K_t = 5$; performance is identical to KL methods for $K_t = 2$, data not shown). We confirm this ratio is a good surrogate for the ARI, which is of course only known in simulation. The Pearson correlation of ratio $\bar{T}_{\text{klar}}/\bar{T}_{\text{klam}}$ and ARI is higher than the correlation of the jump statistic J and ARI in 54% of the simulation conditions (60% for iJ and 69% for hJ). It is more correlated with ARI than KL in 73% of the simulation conditions (77% iKL and 83% hKL). It is more challenging to assess the performance of the methods on real data, where it is not clear k -modes is the correct model. Ranking the DM, J and KL statistics by their correlation with ARI, DM was ranked first once, J was ranked first twice and KL was ranked first three times. The average ranking of KL was higher than DM and J, which shared equal average ranking across all six real datasets.

IV. CONCLUSIONS

We have devised a novel k -modes algorithm, optimal transfer and quick transfer (OTQT), inspired by the k -means algorithm of [11]. We prove the novel algorithm is capable of progressing to a lower value of the objective function even when the competing algorithm would terminate. On real and simulated data, we demonstrate that it is, in fact, more likely to achieve a better optimum given a single initialization. Both the novel and original algorithms share $O(npK)$ run time per iteration [11]. However, the proposed algorithm is computationally slower than the existing algorithm [15] per iteration, yet it appears to scale better with complexity in the data, including more coordinates, more difficult clustering, and more clusters. The previous algorithm can be faster under specialized conditions, such as when the clusters are well-separated and the assumed number

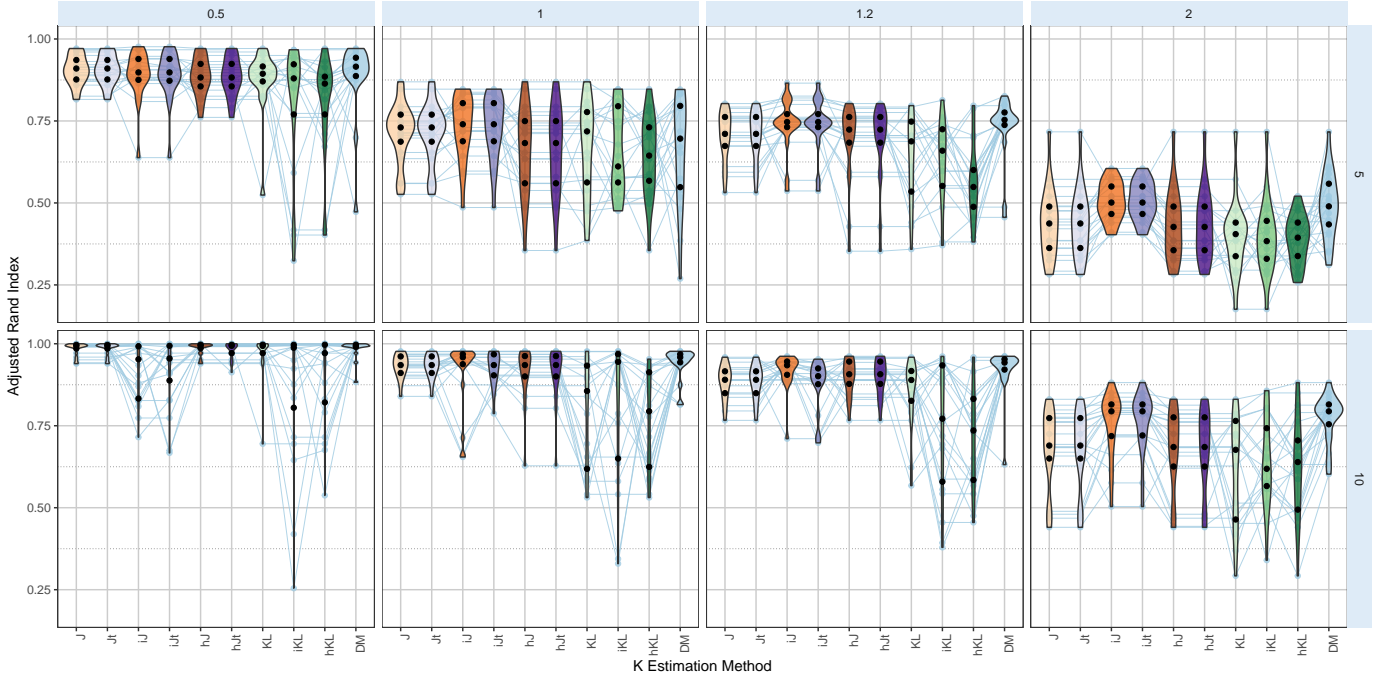


Fig. 7. Adjusted Rand Index (ARI) of solutions reaching target minimum at the \hat{K}_t chosen by each method J, J_t , iJ , iJ_t , hJ , hJ_t , KL, iKL, hKL, and DM. Black dots are quartiles; lines connect results for identical simulations.

of clusters is near the truth, but the absolute difference in time is typically small. In addition, an alternative algorithm (OT) that dispenses with the quick-transfer stage appears to hold promise, performing nearly as well, but slightly faster than the full version of our algorithm. In polishing the algorithm description for publication, we also identified a possible improvement for the OT stage. Currently, when a transfer happens, the second closest mode is set to the previous mode, but the algorithm has information about closer modes if they exist. Thus, further tweaks to the algorithm and more efficient coding may further enhance the temporal advantage of the new algorithm.

Both k -means and k -modes are local optimizers and very sensitive to initialization. There have been many proposed k -modes initialization methods other than the five we implemented [24], [40]–[48]. Some of these methods require all pairwise similarities or distances, making them more computationally complex than the k -modes algorithm itself [42], [48]. Another prioritizes determinism over optimization of the objective function [44]. Some methods are strikingly complicated though still scalable. [40] extend the k -means initialization method of [49] to categorical data. [47] use the clusterings induced by each, perhaps screened, attribute to initialize k -modes, combine the solutions into K consensus clusters, whose modes then form the final initial modes. Several methods are similar to [30] (randomized as **clbr** here), including that of [45], which has been proven a less efficient implementation of Cao et al.’s method [46], [48]. [24], with improvements in [46], choose the first initial mode to have maximum density and subsequent modes to be both dense and distant from previous modes. [48] measure “outlierness” of candidate modes and choose observations with low outlierness and high distance to previous modes. Two other methods are deterministic versions of our **km++** adaptation of k -means++ [41], [43]. The former starts by picking the two most distant observations, the latter the one observation closest to the global mode, and the remaining initial modes are selected to be maximally distant from already chosen modes. Distance is either entropy [41] or Hamming distance [43]. Other algorithms have been proposed to improve optimization of the k -modes objective function without repeated reinitialization, including a tabu search [50], a genetic algorithm [51], a partial swarm optimizer [52], an artificial bee colony optimizer [39] and a Cuckoo search [53]. Most global optimizers and some initializers employ the traditional k -modes algorithms within their approach, and hence could benefit from use of the OTQT or OT algorithms. Our five stochastic initialization methods include random initialization (**klar**), which is the most popular initializer in k -modes implementations. While we found specialized initialization methods can be more accurate than **klar**, notably **km++** and **clbr**, especially for $K < K_t$ (Fig. 13), they were computationally more expensive and could not beat **klar** in ultimate speed to the optimum (Fig. 5).

There has been relatively little work on detecting the true number of clusters K_t for categorical data. We adapted and modified two statistics for estimating K_t from the k -means literature, the jump statistic [32] and the ratio of [33] (KL statistic). There is little theory to support the use of either statistic, particularly in the case of categorical data. The number of independent coordinates p plays a role in these statistics, but it is not clear what the true number of coordinates should be for categorical data. It is not unusual to expand categorical data to use one indicator variable per category, which greatly increases p [54]. In addition, the theory assumes equal cluster sizes. We proposed two weighting schemes to retrospectively adjust the optimized

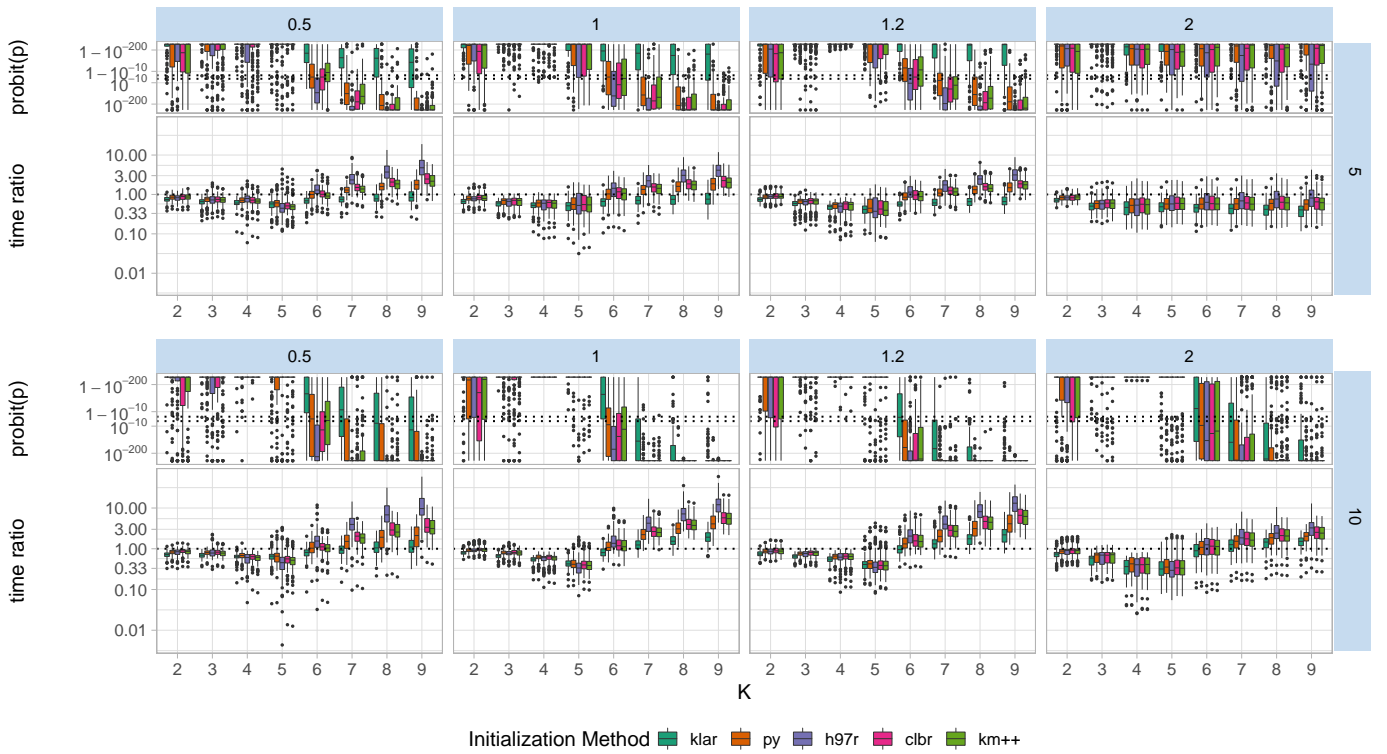


Fig. 8. Timing comparison for mode update vs. no mode update during initialization at $K_t = 5$ with algorithm H97. Each initialization method is run from the same K initial modes with or without mode updates during the first iteration and the real time to reach the target is recorded. See Fig. 4 legend for further details.

objective function before its use in the jump or KL statistic as an attempt to correct for this assumption. Weighting the jump statistic (iJ) by the inverse mean cluster size can improve performance when there is high overlap, but it hurts performance when clusters are well separated. When successful, it appears to identify additional, valid clusters missed by the unweighted jump statistic, but it may also produce support for invalid clusters. We propose a novel DM method for estimating the number of clusters based on the relative time to a target optimum for initialization methods with or without update during the first iteration. The method is based on the observation that updates to the initial modes during the first iteration hurt the optimizer specifically when estimation $K > K_t$ (Fig. 8). The timing differences pinpoint the true K_t more accurately and consistently than any of the theory-based methods (Table IV).

We did find two K estimation methods specifically designed for categorical clustering. [55] develop a method that uses the minimum expected entropy to estimate K . Briefly, after obtaining the minimum expected entropy, or a good approximation, as a function of K , they choose \hat{K}_t to be the choice that maximizes the second-order central finite difference of the minimum expected entropy. Use of the second-order difference is reminiscent of the KL criterion, which maximizes a ratio of finite differences. However, since minimizing the expected entropy is equivalent to maximizing the likelihood over a hard-clustering of observations assumed to have independent multinoulli-distributed coordinates [56], this method assumes a distinct model from that of k -modes (although very similar to our simulation model). [24] propose a method to choose K that is intimately linked to their initialization method. While we implemented neither their initialization method nor K selection method, we note that their method identified $\hat{K}_t = 2$ clusters for the mushroom data, $\hat{K}_t = 4$ or 7 clusters for the zoo data, and $\hat{K}_t = 4$ clusters for the soybean data, which compares well with DM and some KL criteria considered here.

The k -modes algorithm is not the only clustering method for categorical data. Most approaches transform the data so that numeric clustering methods can apply [14], [54], [57]. Such approaches include defining a distance [17], [18], [26], [58]–[62] or similarity [19], [27], [63]–[66] or link [67] for categorical data and using the result in an appropriate clustering algorithm. Others optimize, often approximately, criteria defined for categorical data [15], [41], [50], [68]–[83]. Each of these methods and k -modes assume, either explicitly or implicitly, some generative model, and while there have been some comparisons of their performance [84], [85], there is no doubt the k -modes objective function is not always the best optimization criteria for categorical data. In many cases, where the generative model is unknown, it may be preferable to employ ensemble methods for combining results from multiple categorical data clustering methods [86]–[89]. Ensemble methods rely on algorithmic efficiency, so when k -modes is included in the ensemble, it will be useful to employ the fastest possible version of the algorithm, such as OTQT and OT. Further, the method could be incorporated in syncytial clustering algorithms for categorical data using Generalized or Gaussianized Distributional Transforms [90], [91] and copula models [92], as outlined in [93].

APPENDIX A SOFTWARE

C code implementing H97, OTQT, and OT, along with all initialization methods, including a greedy version of **km++**, is available at <https://github.com/DormanLab/kmodes>.

APPENDIX B SUPPLEMENTARY FIGURES

Here we include supplementary figures for additional analyses that are mentioned but not displayed in the main text. The figures are ordered as they are referenced in the main text. The main text focuses on the comparison of algorithms H97 and OTQT, but here we show there are smaller, but sometimes significant differences between the OTQT and OT algorithms. Similarly, the main text focuses on results for simulation data with $K_t = 5$, but similar patterns are found for the $K_t = 2$ simulations. In Figs. 9, 11 and 12, we compare OTQT and OT in terms of the number and timing of initializations reaching the target for the real data, $K_t = 2$ simulation data, and $K_t = 5$ simulation data. Fig. 10 shows the accuracy and timing results for comparing algorithms H97 and OTQT for $K_t = 2$ simulation data. We focused on the ranking of initialization by time to target in the main text, but we also compared the ranking of initialization methods by accuracy per initialization run. Fig. 13 shows rankings by accuracy for the $K_t = 5$ simulation data, and Fig. 14 shows ranking by both accuracy and time for the $K_t = 2$ simulation data. Detailed effect sizes are displayed for pairs of initialization methods in Fig. 15 for $K_t = 5$ simulations and Fig. 16 for $K_t = 2$ simulations.

REFERENCES

- [1] D. B. Ramey, "Nonparametric clustering techniques," in *Encyclopedia of Statistical Science*. New York: Wiley, 1985, vol. 6, pp. 318–319.
- [2] G. J. McLachlan and K. E. Basford, *Mixture Models: Inference and Applications to Clustering*. New York: Marcel Dekker, 1988.
- [3] L. Kaufman and P. J. Rousseeuw, *Finding Groups in Data*. New York: John Wiley & Sons, 1990.
- [4] B. S. Everitt, S. Landau, and M. Leesem, *Cluster Analysis (4th ed.)*. New York: Hodder Arnold, 2001.
- [5] V. Melnykov and R. Maitra, "Finite mixture models and model-based clustering," *Statistics Surveys*, vol. 4, pp. 80–116, 2010.
- [6] R. Xu and D. C. Wunsch, *Clustering*. NJ, Hoboken: John Wiley & Sons, 2009.
- [7] C. Bouveyron, G. Celeux, T. B. Murphy, and A. E. Raftery, *Model-based clustering and classification for data science: with applications in R*, ser. Statistical and Probabilistic Mathematics. New York, NY : Cambridge University Press, 2019.
- [8] R. J. Jancey, "Multidimensional group analysis," *Australian Journal Botany*, vol. 14, pp. 127–130, 1966.
- [9] J. MacQueen, "Some methods for classification and analysis of multivariate observations," *Proceedings of the Fifth Berkeley Symposium*, vol. 1, pp. 281–297, 1967.
- [10] S. Lloyd, "Least squares quantization in PCM," *Information Theory, IEEE Transactions on*, vol. 28, no. 2, pp. 129–137, 1982.
- [11] J. A. Hartigan and M. A. Wong, "A K-means clustering algorithm," *Applied Statistics*, vol. 28, no. 1, pp. 100–108, 1979.
- [12] B. Andreopoulos, *Data Clustering Algorithms and Applications*. Boca Raton, Fla.: CRC Press, 2014, ch. 12, pp. 277–304.
- [13] M. Á. Carreira-Perpiñán and W. Wang, "The K-modes algorithm for clustering," 2013.
- [14] A. Chaturvedi, P. E. Green, and J. D. Carroll, "K-modes clustering," *Journal of Classification*, vol. 18, no. 1, pp. 35–55, 2001.
- [15] Z. Huang, "A fast clustering algorithm to cluster very large categorical data sets in data mining," in *Proceedings of the SIGMOD Workshop on Research Issues on Data Mining and Knowledge Discovery*. Department of Computer Science, The University of British Columbia, Canada, 1997, pp. 1–8.
- [16] S. Z. Selim and M. A. Ismail, "K-means-type algorithms: A generalized convergence theorem and characterization of local optimality," *IEEE Transactions on Pattern Analysis and Machine Intelligence*, vol. 6, no. 1, pp. 81–87, 1984.
- [17] M. K. Ng, M. J. Li, J. Z. Huang, and Z. He, "On the impact of dissimilarity measure in K-modes clustering algorithm," *IEEE Transactions on Pattern Analysis and Machine Intelligence*, vol. 29, no. 1, pp. 503–507, 2007.
- [18] F. Cao, J. Liang, D. Li, L. Bai, and C. Dang, "A dissimilarity measure for the K-modes clustering algorithm," *Knowledge-Based Systems*, vol. 26, pp. 120 – 127, 2012.
- [19] R. S. Sangam and H. Om, "The K-modes algorithm with entropy based similarity coefficient," *Procedia Computer Science*, vol. 50, pp. 93 – 98, 2015.
- [20] M. García-Magariños and J. A. Vilar, "A framework for dissimilarity-based partitioning clustering of categorical time series," *Data Mining and Knowledge Discovery*, vol. 29, no. 2, pp. 466–502, 2015.
- [21] S. Har-Peled and B. Sadri, "How fast is the K-means method?" *Algorithmica*, vol. 41, no. 3, pp. 185–202, 2005.
- [22] M. Telgarsky and A. Vattani, "Hartigan's method: K-means clustering without Voronoi," in *Proceedings of the Thirteenth International Conference on Artificial Intelligence and Statistics*, ser. Proceedings of Machine Learning Research, Y. W. Teh and M. Titterton, Eds., vol. 9. Chia Laguna Resort, Sardinia, Italy: PMLR, 13–15 May 2010, pp. 820–827.
- [23] J. A. Hartigan, *Clustering algorithms*. New York: Wiley, 1975.
- [24] L. Bai, J. Liang, and C. Dang, "An initialization method to simultaneously find initial cluster centers and the number of clusters for clustering categorical data," *Knowledge-Based Systems*, vol. 24, no. 6, pp. 785 – 795, 2011.
- [25] Z. He, X. Xu, and S. Deng, "Attribute value weighting in K-modes clustering," *Expert Systems with Applications*, vol. 38, no. 12, pp. 15365–15369, 2011.
- [26] J. Kim and L. Billard, "Dissimilarity measures and divisive clustering for symbolic multimodal-valued data," *Computational Statistics & Data Analysis*, vol. 56, no. 9, pp. 2795 – 2808, 2012.
- [27] T. R. dos Santos and L. E. Zárate, "Categorical data clustering: What similarity measure to recommend?" *Expert Systems with Applications*, vol. 42, no. 3, pp. 1247 – 1260, 2015.
- [28] K. Kim, "A weighted K-modes clustering using new weighting method based on within-cluster and between-cluster impurity measures," *Journal of Intelligent & Fuzzy Systems*, vol. 32, no. 1, pp. 979–990, 2017.
- [29] N. de Vos, "Python K-modes, version 0.8," <https://github.com/nicodv/kmodes>, 2017.
- [30] F. Cao, J. Liang, and L. Bai, "A new initialization method for categorical data clustering," *Expert Systems with Applications*, vol. 36, no. 7, pp. 10223 – 10228, 2009.
- [31] D. Arthur and S. Vassilvitskii, "K-means++: the advantages of careful seeding," in *Proceedings of the Eighteenth Annual ACM-SIAM Symposium on Discrete Algorithms*, ser. SODA '07. Philadelphia, PA, USA: Society for Industrial and Applied Mathematics, 2007, pp. 1027–1035.
- [32] C. A. Sugar and G. M. James, "Finding the number of clusters in a dataset," *Journal of the American Statistical Association*, vol. 98, no. 463, pp. 750–763, 2003.

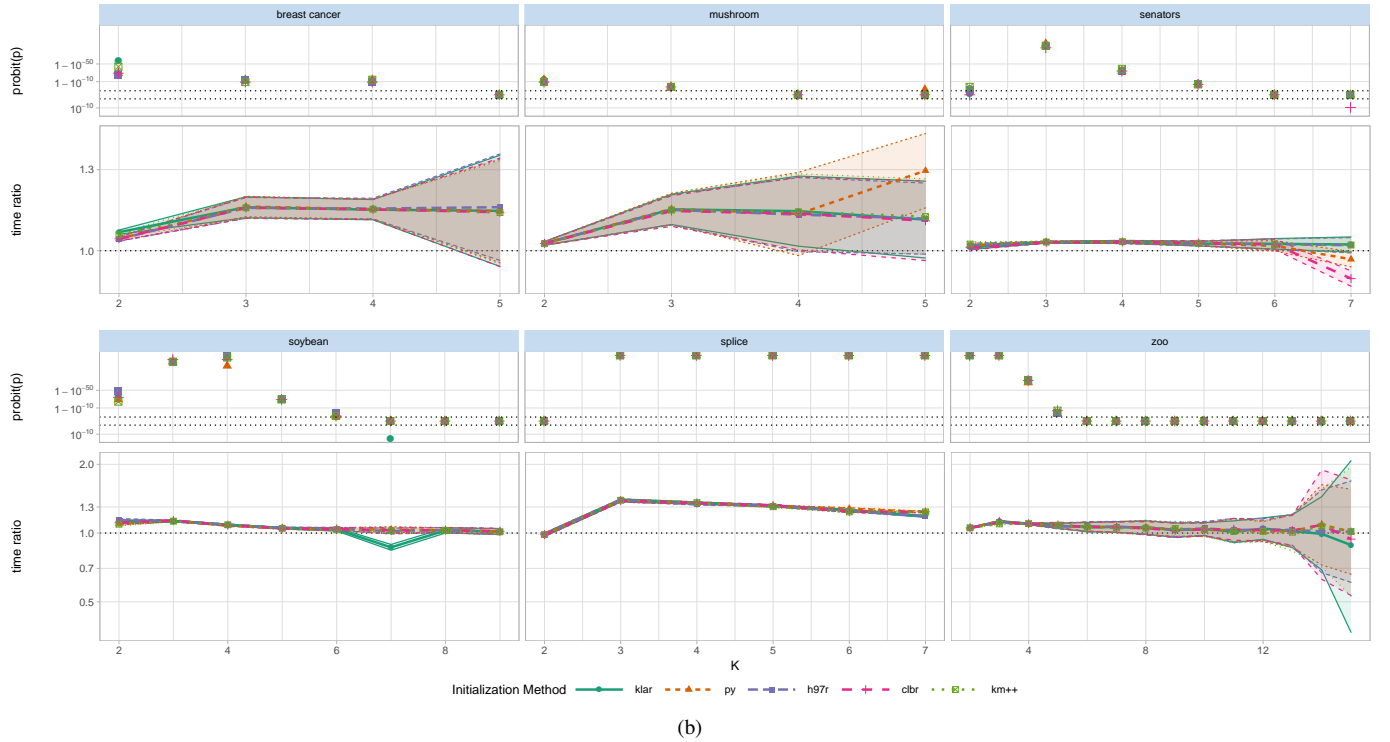
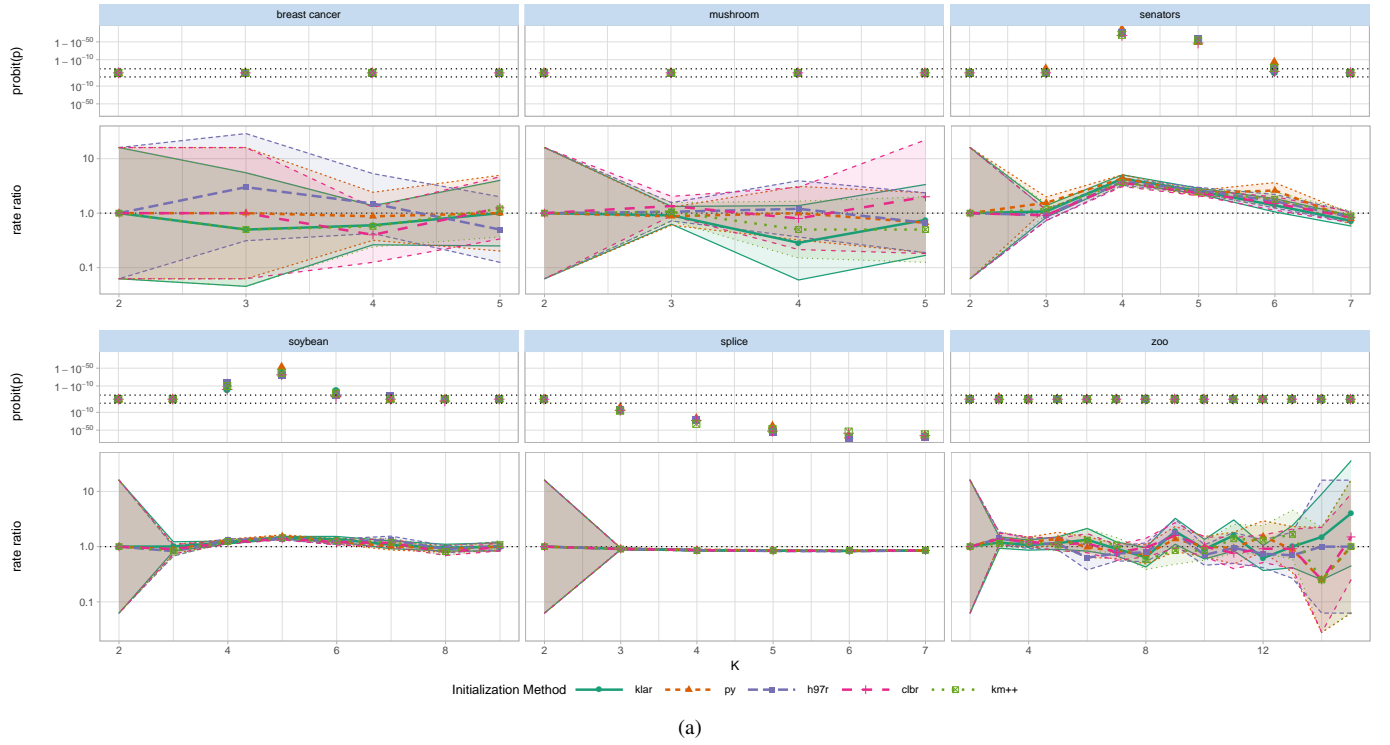


Fig. 9. Comparison of OTQT and OT on achieving target minimum. See Fig. 3 legend for further explanation.

- [33] W. J. Krzanowski and Y. T. Lai, "A criterion for determining the number of groups in a data set using sum-of-squares clustering," *Biometrics*, vol. 44, no. 1, pp. 23–34, 1988.
- [34] L. Hubert and P. Arabie, "Comparing partitions," *Journal of Classification*, vol. 2, pp. 193–218, 1985.
- [35] M. Lichman, "UCI machine learning repository," 2013. [Online]. Available: <http://archive.ics.uci.edu/ml>
- [36] O. Banerjee, L. E. Ghaoui, and A. d'Aspremont, "Model selection through sparse maximum likelihood estimation for multivariate Gaussian or binary data," *Journal of Machine Learning Research*, vol. 9, no. Mar, pp. 485–516, 2008.
- [37] S. Holm, "A simple sequentially rejective multiple test procedure," *Scandinavian Journal of Statistics*, vol. 6, no. 2, pp. 65–70, 1979.
- [38] E. C. Fieller, "Some problems in interval estimation," *Journal of the Royal Statistical Society, Series B*, vol. 16, no. 2, pp. 175–185, 1954.
- [39] J. Ji, W. Pang, Y. Zheng, Z. Wang, and Z. Ma, "A novel artificial bee colony based clustering algorithm for categorical data," *PLOS ONE*, vol. 10, no. 5,

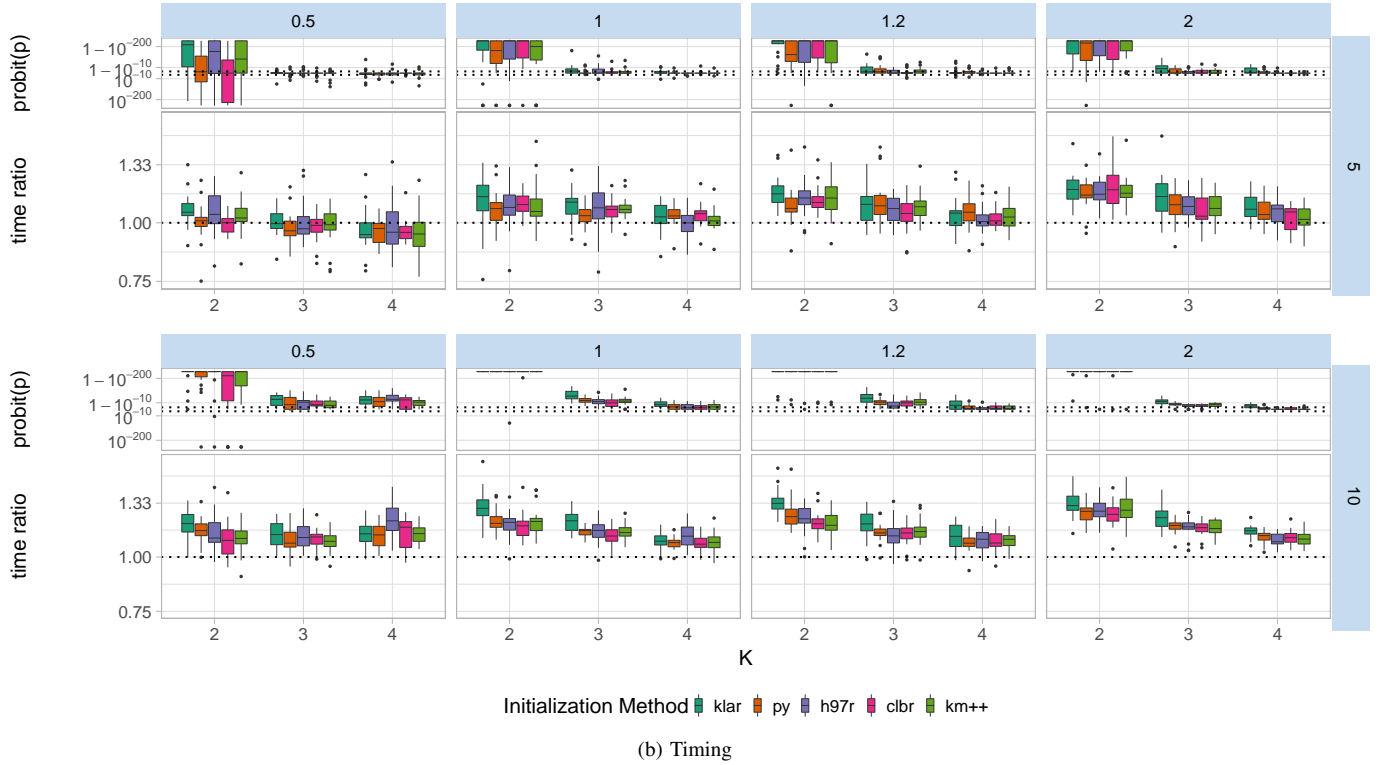
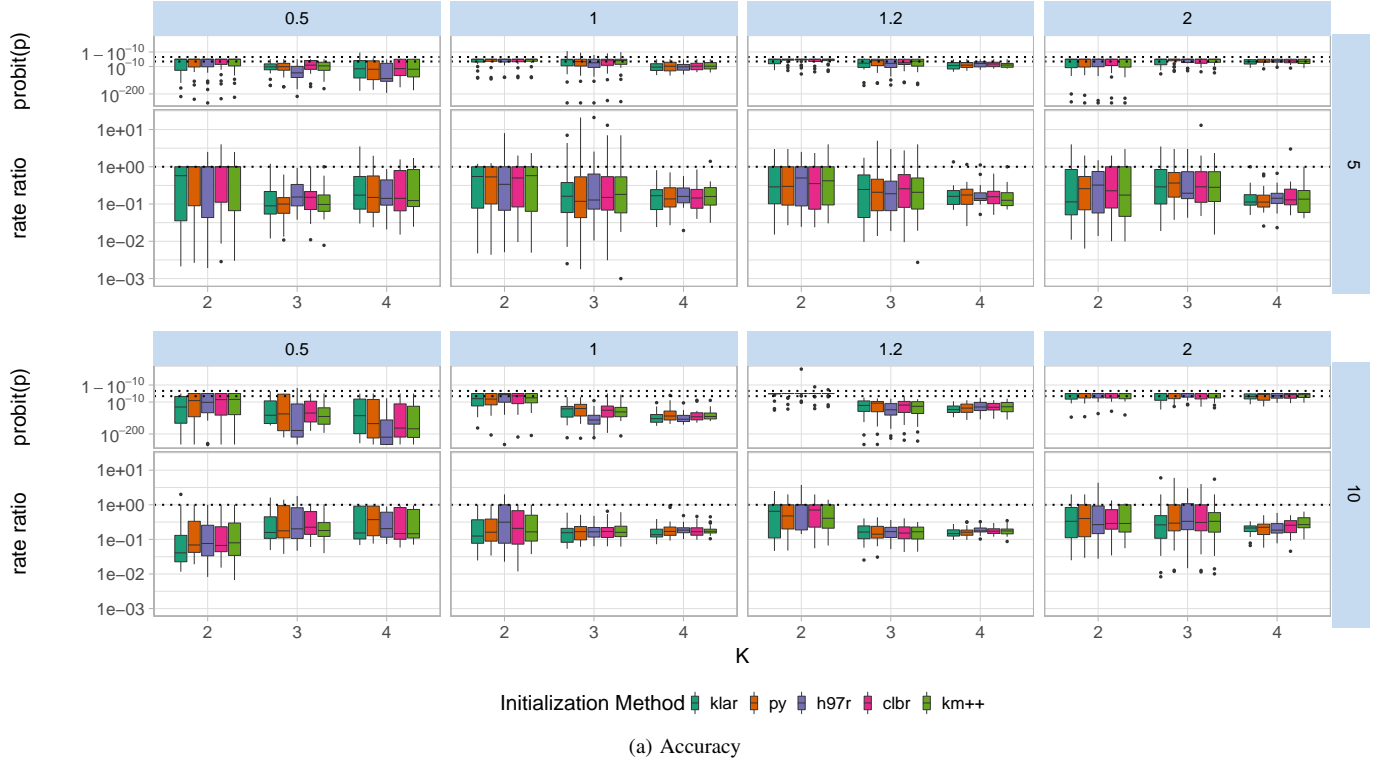


Fig. 10. Accuracy and timing of H97 vs. OTQT for $K_t = 2$. See Fig. 4 legend for further explanation.

p. e0127125, 2015.

- [40] Y. Sun, Q. Zhu, and Z. Chen, “An iterative initial-points refinement algorithm for categorical data clustering,” *Pattern Recognition Letters*, vol. 23, no. 7, pp. 875 – 884, 2002.
- [41] D. Barab  , Y. Li, and J. Couto, “COOLCAT: an entropy-based algorithm for categorical clustering,” in *Proceedings of the Eleventh International Conference on Information and Knowledge Management*, ser. CIKM ’02. Association for Computing Machinery, 2002, pp. 582–589.
- [42] S. S. Khan and A. Ahmad, “Computing initial points using density based multiscale data condensation for clustering categorical data,” in *Proceedings of the 2nd International Conference on Applied Artificial Intelligence (ICAAI)*, 2003.
- [43] Z. He, “Farthest-point heuristic based initialization methods for K-modes clustering,” 2006.

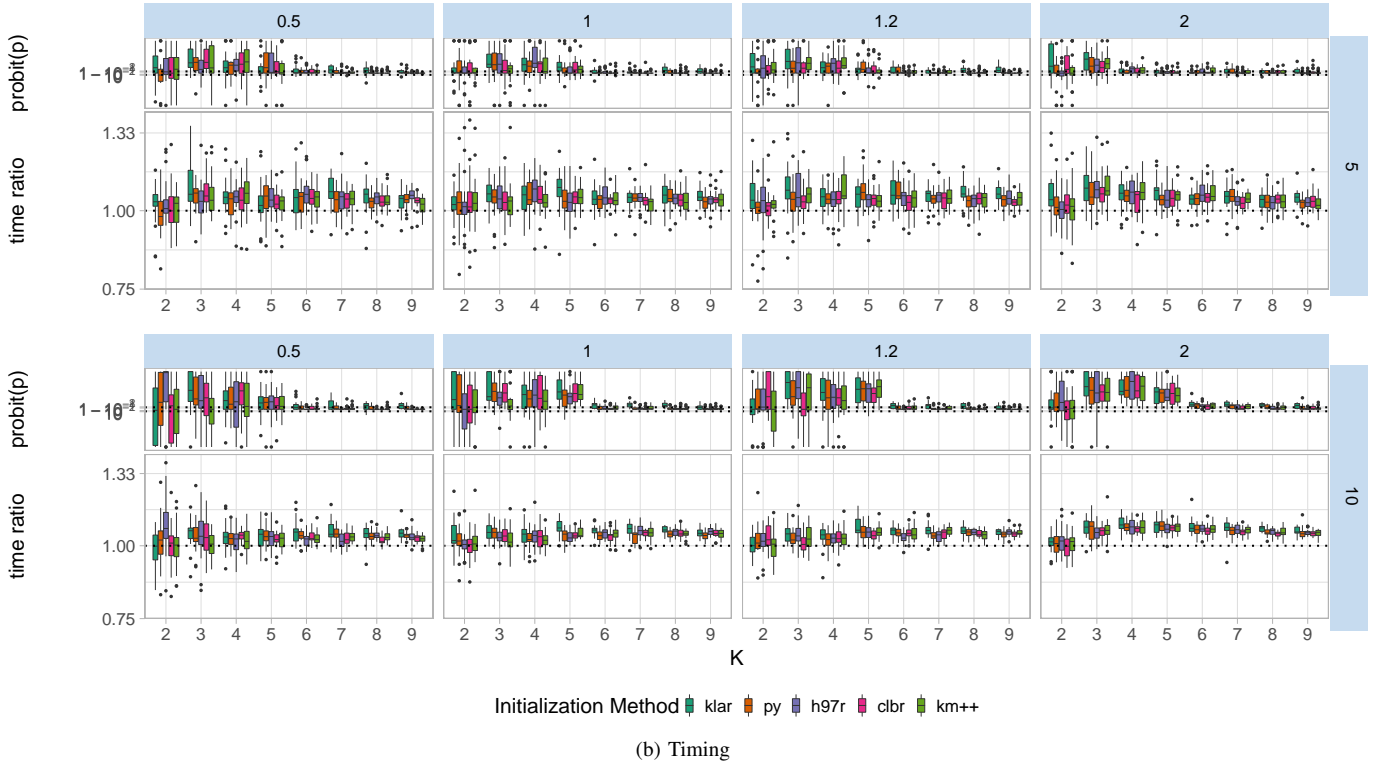
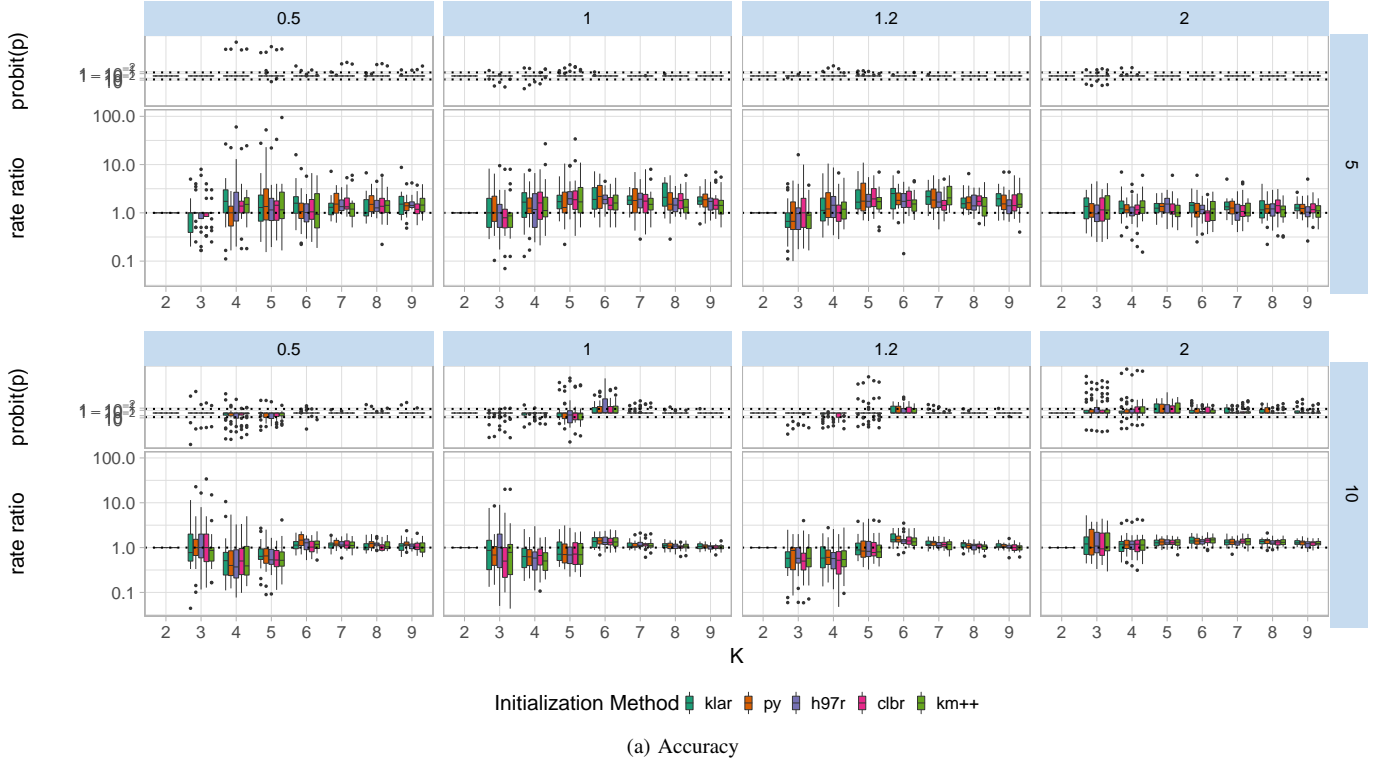


Fig. 11. Accuracy and timing of OTQT vs. OT for $K_t = 5$. See Fig. 4 legend for further explanation.

- [44] S. S. Khan and S. Kant, "Computation of initial modes for K-modes clustering algorithm using evidence accumulation," in *Proceedings of the 20th International Joint Conference on Artificial Intelligence*, ser. IJCAI, 2007, pp. 2784–2789.
- [45] S. Wu, Q. Jiang, and J. Z. Huang, "A new initialization method for clustering categorical data," in *Advances in Knowledge Discovery and Data Mining*, Z.-H. Zhou, H. Li, and Q. Yang, Eds. Springer Berlin Heidelberg, 2007, pp. 972–980.
- [46] L. Bai, J. Liang, C. Dang, and F. Cao, "A cluster centers initialization method for clustering categorical data," *Expert Systems with Applications*, vol. 39, no. 9, pp. 8022 – 8029, 2012.
- [47] S. S. Khan and A. Ahmad, "Cluster center initialization algorithm for K-modes clustering," *Expert Systems with Applications*, vol. 40, no. 18, pp. 7444–7456, 2013.

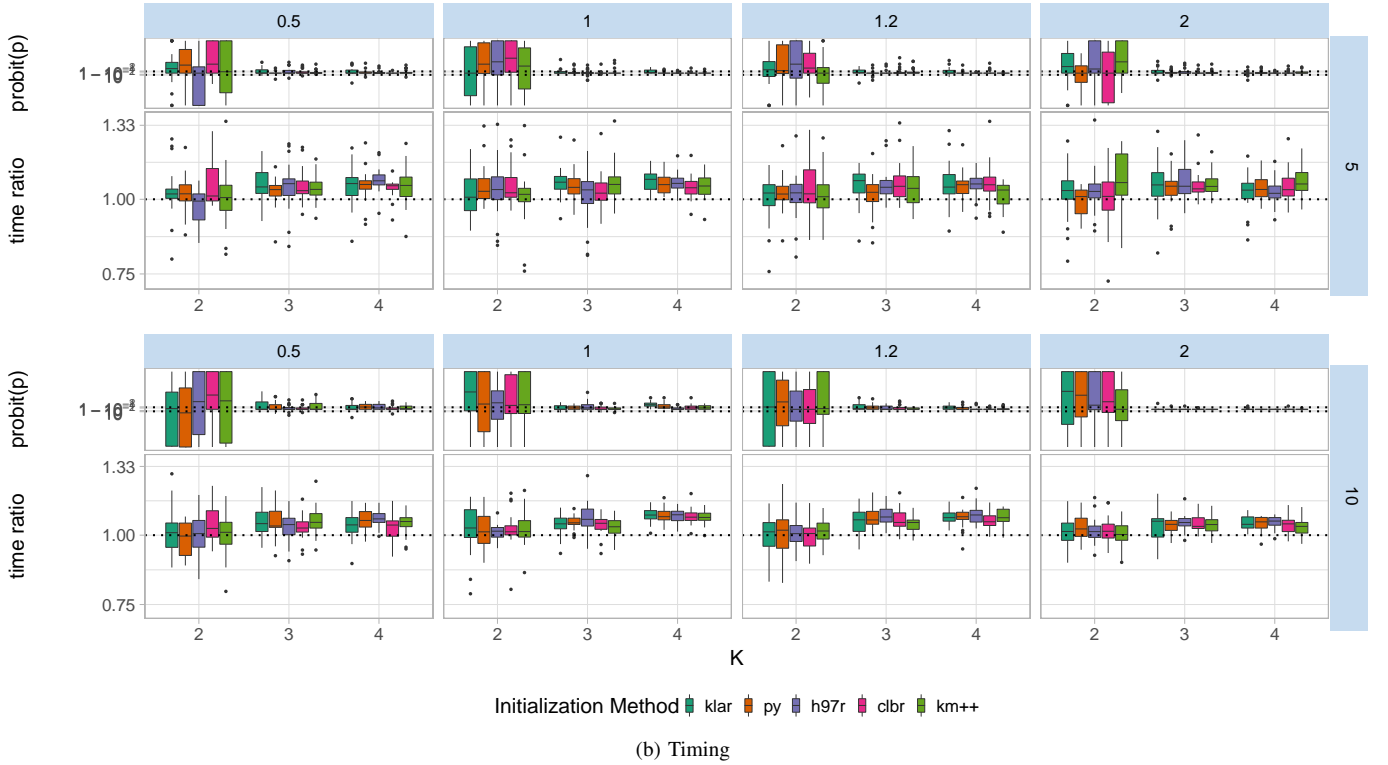
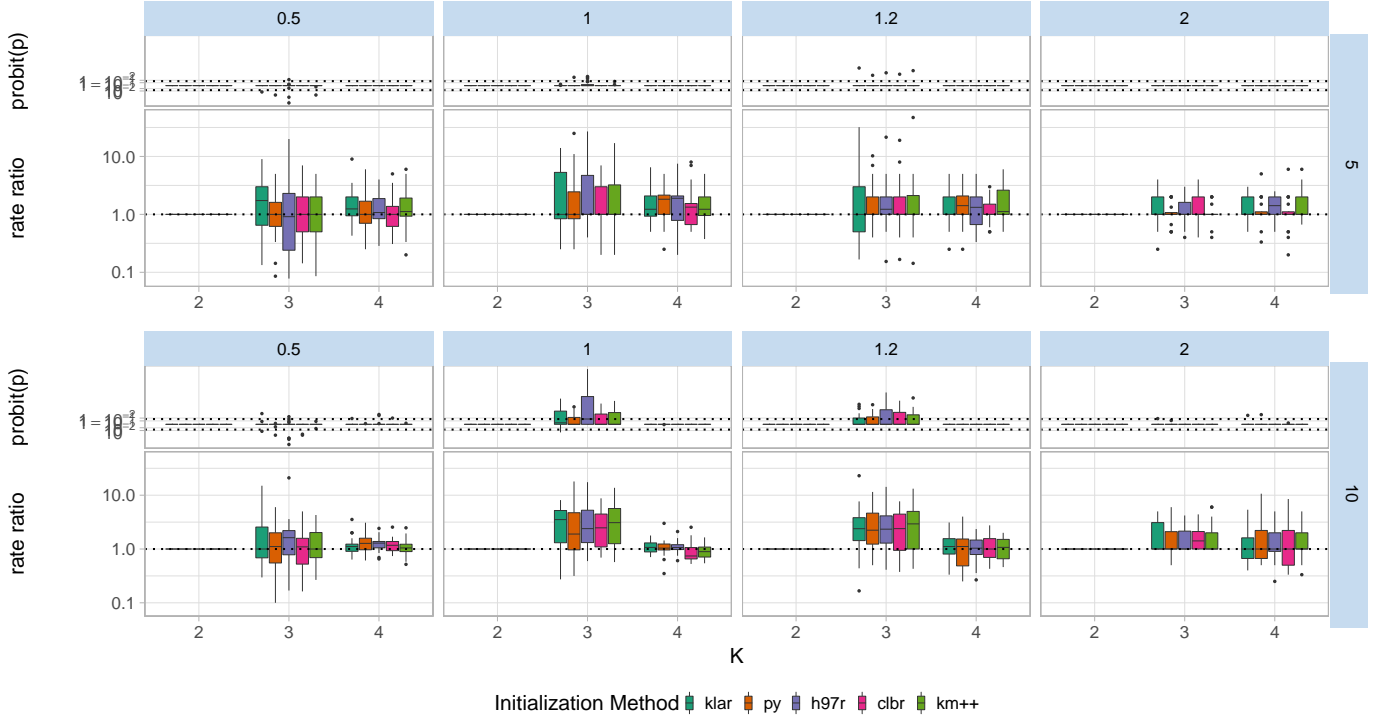


Fig. 12. Accuracy and timing of OTQT vs. OT for $K_t = 2$. See Fig. 4 legend for further explanation.

- [48] F. Jiang, G. Liu, J. Du, and Y. Sui, "Initialization of K-modes clustering using outlier detection techniques," *Information Sciences*, vol. 332, pp. 167–183, 2016.
- [49] P. S. Bradley and U. M. Fayyad, "Refining initial points for K-means clustering," in *Proceedings of the 15th International Conference on Machine Learning*, 1998, pp. 91–99.
- [50] R. T. Ng and J. Han, "CLARANS: a method for clustering objects for spatial data mining," *IEEE Transactions on Knowledge and Data Engineering*, vol. 14, no. 5, pp. 1003–1016, 2002.
- [51] G. Gan, Z. Yang, and J. Wu, *A Genetic K-Modes Algorithm for Clustering Categorical Data*. Springer, 2005, vol. 3584, pp. 195–202.
- [52] H. Izakian, A. Abraham, and V. Snasel, "Clustering categorical data using a swarm-based method," in *World Congress on Nature & Biologically Inspired*

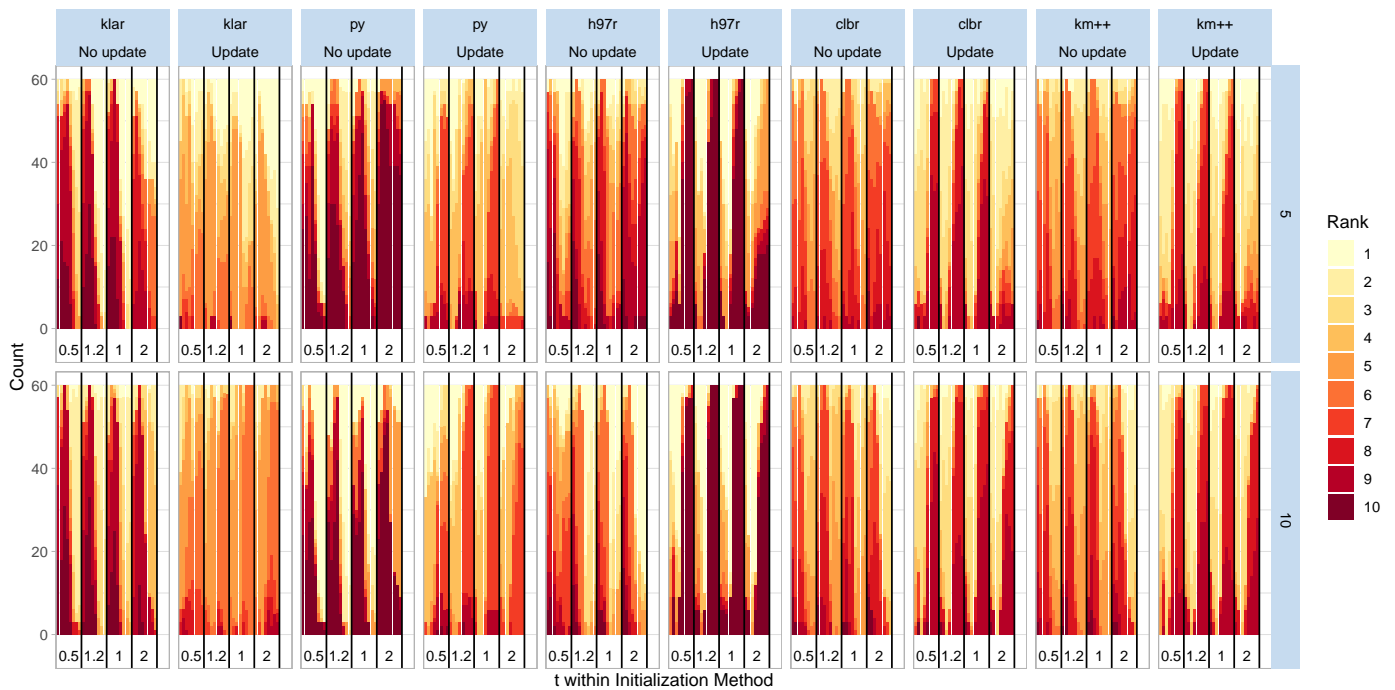


Fig. 13. Comparison of five initialization methods using algorithm H97 on simulated data $K_t = 5$. In contrast to Fig. 13, the initialization methods are ranked by number of initializations achieving the target minimum.

Computing. IEEE Computer Society, 2009, pp. 1720–1724.

- [53] K. Lakshmi, V. Karthikeyani, S. Shanthi, and S. Parvathavarthini, “Clustering categorical data using K-modes based on cuckoo search optimization algorithm,” *ICTACT Journal on Soft Computing*, vol. 8, no. 1, pp. 1561–1566, 2017.
- [54] H. Ralambondrainy, “A conceptual version of the K-means algorithm,” *Pattern Recognition Letters*, vol. 16, no. 11, pp. 1147–1157, 1995.
- [55] K. Chen and L. Liu, ““Best K”: critical clustering structures in categorical datasets,” *Knowledge and Information Systems*, vol. 20, no. 1, pp. 1–33, 2009.
- [56] T. Li, S. Ma, and M. Ogihara, “Entropy-based criterion in categorical clustering,” in *Proceedings of the Twenty-First International Conference on Machine Learning*, ser. ICML 04. Association for Computing Machinery, 2004, pp. 68–75.
- [57] J. D. Carroll, P. E. Green, and C. M. Schaffer, “Interpoint distance comparisons in correspondence analysis,” *Journal of Marketing Research*, vol. 23, no. 3, pp. 271–280, 1986.
- [58] K. C. Gowda and E. Diday, “Symbolic clustering using a new dissimilarity measure,” *Pattern Recognition*, vol. 24, no. 6, pp. 567–578, 1991.
- [59] D. Ienco, R. G. Pensa, and R. Meo, “From context to distance: Learning dissimilarity for categorical data clustering,” *ACM Transactions on Knowledge Discovery from Data*, vol. 6, no. 1, pp. 1–25, 2012.
- [60] H. Jia, Y. Cheung, and J. Liu, “A new distance metric for unsupervised learning of categorical data,” *IEEE Transactions on Neural Networks and Learning Systems*, vol. 27, no. 5, pp. 1065–1079, 2016.
- [61] S. Q. Le and T. B. Ho, “An association-based dissimilarity measure for categorical data,” *Pattern Recognition Letters*, vol. 26, no. 16, pp. 2549 – 2557, 2005.
- [62] H. Zhou, Y. Zhang, and Y. Liu, “A global-relationship dissimilarity measure for the K-modes clustering algorithm,” *Computational Intelligence and Neuroscience*, vol. 2017, p. 7, 2017.
- [63] D. W. Goodall, “A new similarity index based on probability,” *Biometrics*, vol. 22, no. 4, pp. 882–907, 1966.
- [64] J. C. Gower, “A general coefficient of similarity and some of its properties,” *Biometrics*, vol. 27, no. 4, pp. 857–874, 1971.
- [65] K. C. Gowda and E. Diday, “Symbolic clustering using a new similarity measure,” *IEEE Transactions on Systems, Man, and Cybernetics*, vol. 22, no. 2, pp. 368–378, 1992.
- [66] A. Ahmad and L. Dey, “A method to compute distance between two categorical values of same attribute in unsupervised learning for categorical data set,” *Pattern Recognition Letters*, vol. 28, no. 1, pp. 110 – 118, 2007.
- [67] S. Guha, R. Rastogi, and K. Shim, “ROCK: A robust clustering algorithm for categorical attributes,” *Information Systems*, vol. 25, no. 5, pp. 345 – 366, 2000.
- [68] P. F. Lazarsfeld, *Studies in Social Psychology in World War II*, ser. Measurement and Prediction. Princeton, NJ: Princeton University Press, 1950, vol. IV, ch. The Logical and Mathematical Foundation of Latent Structure Analysis, pp. 362–412.
- [69] L. A. Goodman, “Exploratory latent structure analysis using both identifiable and unidentifiable models,” *Biometrika*, vol. 61, no. 2, pp. 215–231, 1974.
- [70] C. C. Clogg and L. A. Goodman, “Latent structure analysis of a set of multidimensional contingency tables,” *Journal of the American Statistical Association*, vol. 79, no. 388, pp. 762–771, 1984.
- [71] V. Ganti, J. Gehrke, and R. Ramakrishnan, “Cactus-clustering categorical data using summaries,” in *Proceedings of the Fifth ACM SIGKDD International Conference on Knowledge Discovery and Data Mining*, ser. KDD ’99. Association for Computing Machinery, 1999, pp. 73–83.
- [72] D. Gibson, J. Kleinberg, and P. Raghavan, “Clustering categorical data: an approach based on dynamical systems,” *The VLDB Journal*, vol. 8, no. 3, pp. 222–236, 2000.
- [73] Z. He, X. Xu, and S. Deng, “Squeezer: An efficient algorithm for clustering categorical data,” *Journal of Computer Science and Technology*, vol. 17, no. 5, pp. 611–624, 2002.
- [74] E. Cesario, G. Manco, and R. Ortale, “Top-down parameter-free clustering of high-dimensional categorical data,” *IEEE Transactions on Knowledge and Data Engineering*, vol. 19, no. 12, pp. 1607–1624, 2007.
- [75] Z. He, X. Xu, and S. Deng, “k-ANMI: A mutual information based clustering algorithm for categorical data,” *Information Fusion*, vol. 9, no. 2, pp. 223 – 233, 2008.

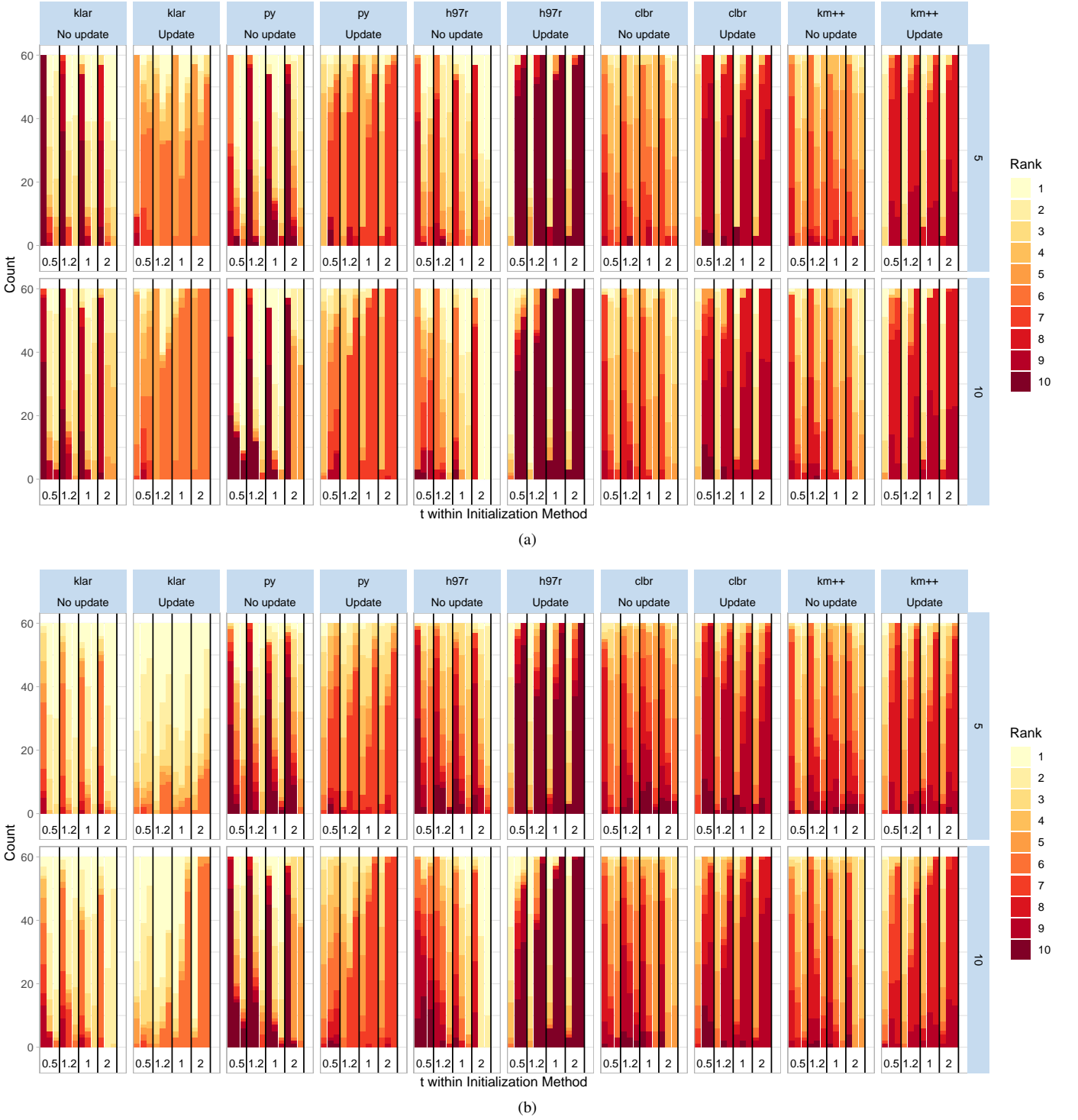


Fig. 14. Comparison of five initialization methods using algorithm H97 on simulated data $K_t = 2$. See Fig. 5 and Fig. 13 legends for further explanation.

- [76] I. Heloulou, M. S. Radjef, and M. T. Kechadi, “A multi-act sequential game-based multi-objective clustering approach for categorical data,” *Neurocomputing*, vol. 267, pp. 320 – 332, 2017.
- [77] P. Andritsos, P. Tsaparas, R. J. Miller, and K. C. Sevcik, “LIMBO: Scalable clustering of categorical data,” in *Advances in Database Technology - EDBT 2004*, E. Bertino, S. Christodoulakis, D. Plexousakis, V. Christophides, M. Koubarakis, K. Böhm, and E. Ferrari, Eds. Springer Berlin Heidelberg, 2004, pp. 123–146.
- [78] M. Li, S. Deng, L. Wang, S. Feng, and J. Fan, “Hierarchical clustering algorithm for categorical data using a probabilistic rough set model,” *Knowledge-Based Systems*, vol. 65, pp. 60 – 71, 2014.
- [79] I.-K. Park and G.-S. Choi, “Rough set approach for clustering categorical data using information-theoretic dependency measure,” *Information Systems*, vol. 48, pp. 289 – 295, 2015.
- [80] D. Parmar, T. Wu, and J. Blackhurst, “MMR: An algorithm for clustering categorical data using rough set theory,” *Data & Knowledge Engineering*, vol. 63, no. 3, pp. 879 – 893, 2007.

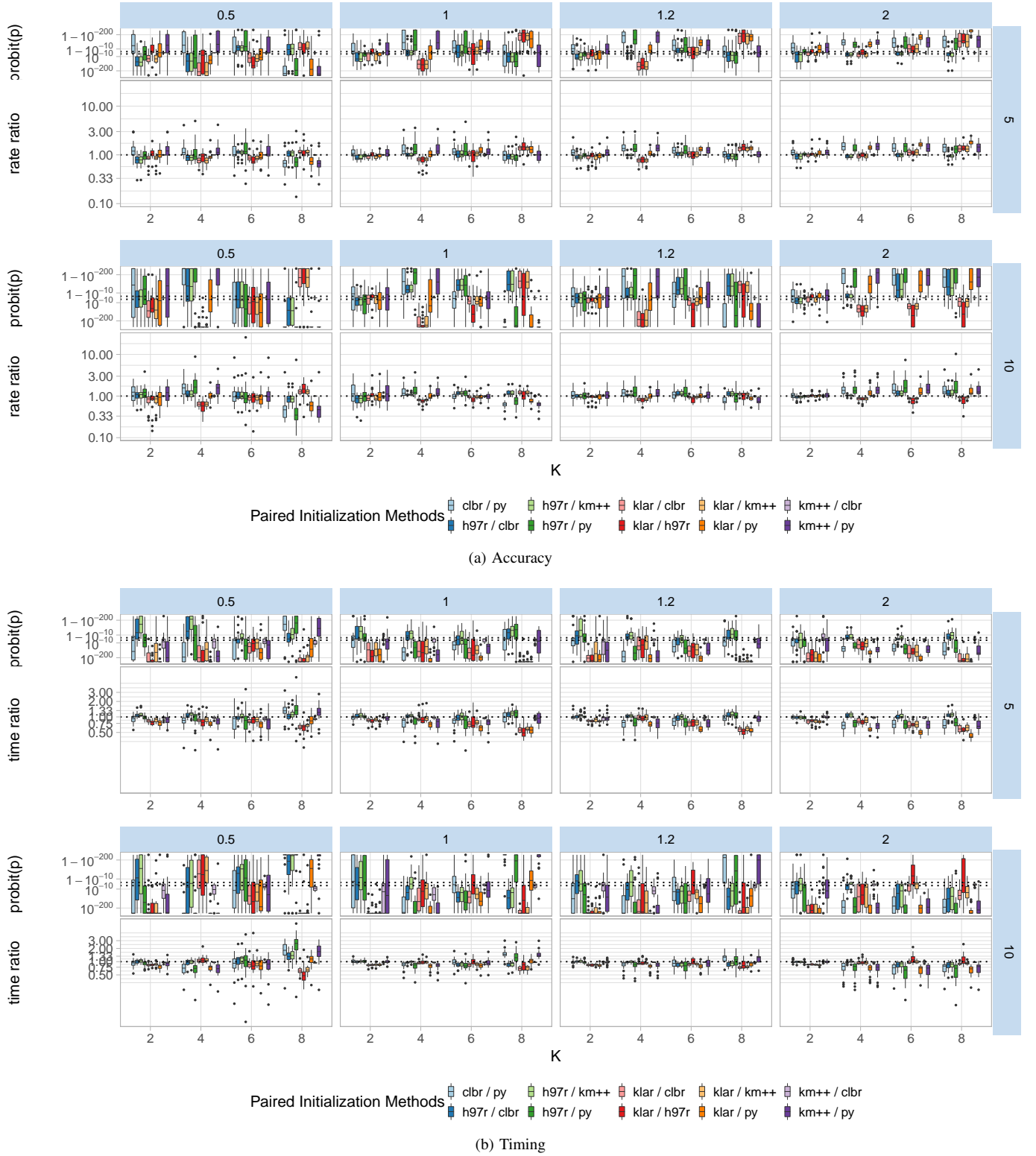


Fig. 15. Pairwise comparison of initialization methods for $K = 5$ under H97.

- [81] A. Sharma and R. Thakur, "GACC: genetic algorithm-based categorical data clustering for large datasets," *International Journal of Data Mining, Modelling and Management*, vol. 9, no. 4, 2017.
- [82] A. K. C. Wong and D. C. C. Wang, "DECA: A discrete-valued data clustering algorithm," *IEEE Transactions on Pattern Analysis and Machine Intelligence*, vol. 1, no. 4, pp. 342–349, 1979.
- [83] P. Zhang, X. Wang, and P. X.-K. Song, "Clustering categorical data based on distance vectors," *Journal of the American Statistical Association*, vol. 101, no. 473, pp. 355–367, 2006.
- [84] L. Anderlucci and C. Hennig, "The clustering of categorical data: A comparison of a model-based and a distance-based approach," *Communications in Statistics - Theory and Methods*, vol. 43, no. 4, pp. 704–721, 2014.

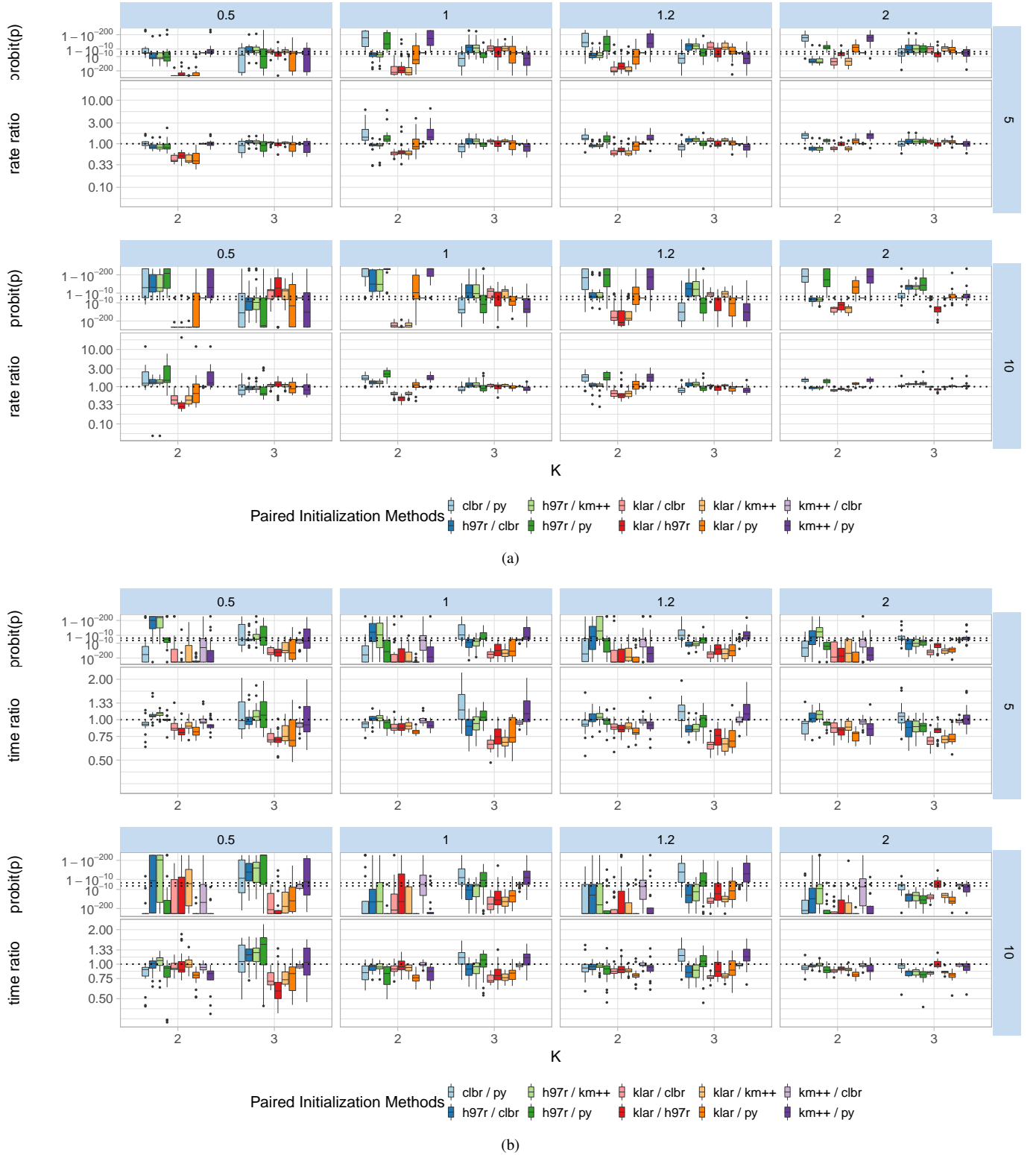


Fig. 16. Pairwise comparison of initialization methods for $K = 2$ under H97.

- [85] L. Bai and J. Liang, "Cluster validity functions for categorical data: a solution-space perspective," *Data Mining and Knowledge Discovery*, vol. 29, no. 6, pp. 1560–1597, 2015.
- [86] Z. He, X. Xu, and S. Deng, "A cluster ensemble method for clustering categorical data," *Information Fusion*, vol. 6, no. 2, pp. 143–151, 2005.
- [87] N. Iam-On, T. Boongeeon, S. Garrett, and C. Price, "A link-based cluster ensemble approach for categorical data clustering," *IEEE Transactions on Knowledge and Data Engineering*, vol. 24, no. 3, pp. 413–425, 2012.
- [88] I. Saha, J. P. Sarkar, and U. Maulik, "Ensemble based rough fuzzy clustering for categorical data," *Knowledge-Based Systems*, vol. 77, pp. 114–127, 2015.
- [89] S. Amiri, B. S. Clarke, and J. L. Clarke, "Clustering categorical data via ensembling dissimilarity matrices," *Journal of Computational and Graphical*

- Statistics*, vol. 27, no. 1, pp. 195–208, 2018.
- [90] L. Rüschendorf, *Mathematical Risk Analysis*. Berlin Heidelberg: Springer-Verlag, 2013.
 - [91] Y. Zhu, F. Dai, and R. Maitra, “Three-dimensional radial visualization of high-dimensional continuous or discrete datasets,” *ArXiv e-prints*, Mar. 2019.
 - [92] R. B. Nelsen, *An Introduction to Copulas*, 2nd ed. New York: Springer, 2006.
 - [93] I. Almodvar-Rivera and R. Maitra, “Kernel-estimated nonparametric overlap-based syncytial clustering,” 2018.